

CSIS Discussion Paper No. 152

Exploratory analysis of the appearance and disappearance of points

Yukio Sadahiro

March 2018

Center for Spatial Information Science, The University of Tokyo

Corresponding author:

Yukio Sadahiro

Center for Spatial Information Science, The University of Tokyo

5-1-5, Kashiwanoha, Kashiwa-shi, Chiba 277-8568, Japan

Phone: +81-471-36-4310

Fax: +81-3-5841-8521

sada@csis.u-tokyo.ac.jp

Abstract

Keywords: appearance, disappearance, point, event, exploratory analysis, visualization

Appearance and disappearance of immovable points are important spatiotemporal events in geographical information science. They represent the birth and death of trees in forests, construction and destruction of buildings in cities, and openings and closures of shops and restaurants. This paper proposes a new exploratory method for analyzing the appearance and disappearance of points. The method helps analysts capturing the overall picture and regional variation of event pattern and detecting distinctive local patterns. Four measures are defined that indicate the intensity of spatial and temporal patterns of events. The measures are visualized as two types of maps called lattice and circle maps. Lattice map directly visualizes the spatial distribution of these measure, which is effective for grasping the overall pattern and its variation. Circle map is useful for detecting distinctive local patterns that may not be easily detectable in lattice map. The proposed method is applied to the analysis of shops and restaurants in Shibuya, Tokyo. Technical soundness of the method is discussed along with empirical findings.

1. Introduction

Appearance and disappearance of immovable points are important spatiotemporal events in geographical information science. They represent the birth and death of trees in forests, construction and destruction of buildings in cities, and openings and closures of shops and restaurants. These events are analyzed in both academic and practical fields. Ecologists analyze the birth and death of plant species to understand the mutual relationship between different species. Geographers and economists analyze the opening and closure of supermarkets to reveal the competitive relationship between retail chains (Scott (1970), Dawson (2012)). Monitoring the spatial and temporal pattern of disease infection is crucial to prevent its expansion (Greene et al. (2016), Carolina et al. (2017)). City planners are concerned with the opening of large shopping centers since it often damages small shops and markets. Event analysis is useful for understanding its underlying structure and forming administrative policies, and thus it has drawn attention of both researchers and administrators.

Analysis of appearances and disappearances generally starts with visual analysis, which helps us grasping the overall picture and local variation of these events (Kovalerchuk and Schwing (2005), Andrienko and Andrienko (2006), Kraak and Ormeling (2011), Lamigueiro (2014), Oyana and Margai (2015)). Events can be visualized as dot map, grid map, and kernel density map. The dot map indicates the exact location of events by using map symbols (Robinson et al. (1995); Dent (1999); Slocum et al. (2009)). The grid map displays the number of events in square cells by color shades (Boots and Csillag 2006). The kernel density map visualizes the density distribution of events calculated by kernel density estimation (Silverman (1986); Scott (2015)). Time series collection of these maps are basic tools for visual exploration of spatiotemporal event pattern.

Analytical method of appearances and disappearances should consider at least four properties of these events. Firstly, these events occur in the spatio-temporal dimension. The temporal pattern of events such as an increase and decrease of appearances needs to be taken into account explicitly. Secondly, the spatial pattern of events depends on that of points on which events can occur. The ratio of events to points is crucial rather than the absolute number of points. Thirdly, the same ratio of events does not always imply the same likelihood. Disappearance of one out of two points is more likely to happen by chance than that of ten out of twenty points. A statistical framework is necessary to address this issue. Fourthly, a close relationship generally exists between appearances and disappearances. They are not totally independent of each other, and consequently, analysis should reveal their relationship as well as their individual patterns.

The dot map does not meet the second and third criteria since they do not directly indicate the event ratio. Analysts have to compare visually the number of events and points, which tends to be unstable and subjective. The grid and kernel density maps, on the other hand, can visualize the ratio of events to points. These maps, however, do not satisfy the third criterion because they do not consider the likelihood of events. Moreover, these maps do not fully meet the fourth criterion. They do not visualize explicitly

the relationship between appearances and disappearances.

To resolve these problems, this paper proposes a new method for analyzing the appearance and disappearance of points. The method aims to support exploratory visual analysis of these events, i.e., to help analysts capturing the overall spatial and temporal pattern and detecting distinctive local patterns. Section 2 discusses related works and literature. Section 3 describes our method for analyzing event pattern. Section 4 applies the proposed method to the analysis of shops and restaurants in Shibuya-ku, Tokyo, Japan. Section 5 summarizes the conclusions with discussion.

2. Related works

Besides the maps mentioned in the previous section, numerous methods have been developed for spatial and spatio-temporal point pattern analysis. This section reviews existing methods closely related to the objective of this paper.

Exploratory statistical methods have been developed in statistics, geography, and epidemiology (Gabriel 2017). Knox and Mantel tests evaluate the spatio-temporal interaction of points (Knox and Bartlett (1964), Mantel (1967), Kulldorff and Hjalmar (1999)). Diggle et al. (1995) and Gabriel and Diggle (2009) employ Ripley's K-function to explore the second-order properties of the point process. Jacquez (1996) extends the nearest-neighbor statistic into spatio-temporal domain to evaluate the spatio-temporal interaction of points. Cronie and Van Lieshout (2015) uses J-function (Van Lieshout and Baddeley (1996), Van Lieshout (2011)) to treat the spatio-temporal point processes.

Detection of spatial and spatio-temporal clusters has also been discussed in the literature. The spatial scan statistic is widely used to detect spatial clusters of points (Naus (1965), Kulldorff and Nagarwalla (1995), Kulldorff (1997), Glaz et al. (2001)). Kulldorff (2001) and Kulldorff et al. (2005) extend the spatial scan statistic to detect spatio-temporal clusters. Kulldorff et al. (2007), Neill (2011), and Neill et al. (2013) propose multivariate scan statistics to treat clusters of multiple types of points. Other methods are also available for cluster detection (Openshaw et al. (1987), Turnbull et al. (1989), Besag and Newell (1991), Fotheringham and Zhan (1996), Conley et al. (2005)).

Estimation of disease risk is an important topic in epidemiology. Relative risk function is generally estimated from the point data of cases and controls by kernel density estimation (Bithell (1991), Kelsall and Diggle (1995), Hazelton and Davies (2009), Fernando et al. (2014), Fernando and Hazelton (2014)). Relative risk function is easily computed by using software package called *sparr* (Davies et al. 2011), and visualized as contour and 3-dimensional maps. When the data are aggregated across spatial units, Bayesian approach is widely used in risk estimation (Clayton and Kaldor (1987), Marshall (1991), Richardson et al. (2004), Lawson (2013)). Bayesian estimation is implemented in GeoDa and *spdep* in R (Anselin et al. (2006), Bivand et al. (2008)), and estimated result is visualized as a choropleth map which is often called disease map.

Spatial birth and death processes represent the appearance and disappearance of points (Preston

(1975), Holley and Stroock (1978), Møller and Sørensen (1994), Moller and Waagepetersen (2003)). Stochastic models have been studied extensively in statistics and theoretical ecology (Finkelshtein et al. (2012), Ovaskainen et al. (2014)). They are used to simulate the appearance and disappearance of points as well as to find their equilibrium state.

Exploratory statistical methods do not fit our purpose since they summarize the spatial and spatio-temporal pattern into numerical measures and functions. Spatial birth and death processes are primarily used for simulating point processes rather than exploratory pattern analysis. A strength of scan statistics and risk estimation is that they explicitly consider the likelihood of events based on a statistical framework. These methods, however, do not evaluate the temporal pattern of events such as an increase and decrease. Moreover, scan statistics focus on cluster detection. They do not fully visualize the overall picture and detailed local variation of event pattern, even if secondary clusters are drawn in maps (Kulldorff et al. (1997), Gangnon and Clayton (2001), Zhang et al. (2010), Li et al. (2011)). Relative risk estimation, on the other hand, does not consider multiple patterns simultaneously. We thus employ the framework of scan statistics with a modification necessary for our setting and purpose. Using the maximum likelihood approach, we develop an exploratory method for analyzing the appearance and disappearance of points.

3. Methods

Suppose there are N points $\Psi = \{P_1, P_2, \dots, P_N\}$ in region S_0 during time period T . Some exist throughout the whole period while others appear or disappear during T . Let $Z_0(\mathbf{x}, r)$ be a circle of radius r centered at location \mathbf{x} . We define cylinder $Z(\mathbf{x}, r)$ as the product of $Z_0(\mathbf{x}, r)$ and T , i.e.,

$$Z(\mathbf{x}, r) = Z_0(\mathbf{x}, r) \otimes T. \quad (1)$$

We denote the cylinder by Z instead of $Z(\mathbf{x}, r)$ for simplicity in the following. Similarly, we define

$$S = S_0 \otimes T. \quad (2)$$

Let $n(Z)$ be the number of points in Z . The following subsections treat the spatial, temporal, and combination of multiple patterns of events successively.

3.1. Spatial pattern

This subsection first considers the spatial pattern of appearances. We evaluate the ratio of appearances to points in Z in comparison with that in $S-Z$ by using the maximum likelihood approach. Let p_0 and q_0 be the probabilities that an appearance occurs in Z and $S-Z$, respectively. The likelihood function is given by

$$L(Z, p_0, q_0) = {}_{n(Z)}C_{a(Z)} p_0^{a(Z)} (1-p_0)^{n(Z)-a(Z)} {}_{n(S-Z)}C_{a(S-Z)} q_0^{a(S-Z)} (1-q_0)^{n(S-Z)-a(S-Z)}, \quad (3)$$

where $a(Z)$ is the number of appearances in Z . The null hypothesis H_0 assumes the same probability of appearance in Z and $S-Z$, i.e., $p_0=q_0$, while the alternative hypothesis H_1 assumes that the probability is different in Z and $S-Z$. The likelihood functions maximized under H_0 and H_1 are given by

$$\begin{aligned} L_0(Z) &= \max_{p_0=q_0} L(Z, p_0, q_0) \\ &= {}_{n(Z)}C_{a(Z)} {}_{n(S-Z)}C_{a(S-Z)} \left(\frac{a(S)}{n(S)} \right)^{a(S)} \left(1 - \frac{a(S)}{n(S)} \right)^{n(S)-a(S)} \end{aligned} \quad (4)$$

and

$$\begin{aligned} L_1(Z) &= \max_{p_0 \neq q_0} L(Z, p_0, q_0) \\ &= {}_{n(Z)}C_{a(Z)} \left(\frac{a(Z)}{n(Z)} \right)^{a(Z)} \left(1 - \frac{a(Z)}{n(Z)} \right)^{n(Z)-a(Z)} {}_{n(S-Z)}C_{a(S-Z)} \left(\frac{a(S-Z)}{n(S-Z)} \right)^{a(S-Z)} \left(1 - \frac{a(S-Z)}{n(S-Z)} \right)^{n(S-Z)-a(S-Z)}, \end{aligned} \quad (5)$$

respectively. The log likelihood ratio is

$$\lambda_A(Z) = \log L_1(Z) - \log L_0(Z). \quad (6)$$

Given \mathbf{x} , we expand circle $Z_0(\mathbf{x}, r)$ from a small one until its radius reaches at a predetermined value r_{\max} to find the maximum value of $\lambda_A(Z)$. Measure $\alpha_A(\mathbf{x})$ is then defined as

$$\alpha_A(\mathbf{x}) = \max_{r \leq r_{\max}} \lambda_A(Z). \quad (7)$$

The above procedure is almost the same as that used in spatial scan statistics. A difference lies in that scan statistics maximize $\lambda_A(Z)$ under the condition $p_0 > q_0$ because their objective is cluster detection. Equation (7) does not impose this condition because our interest lies in the overall spatial pattern of appearances. Measure $\alpha_A(\mathbf{x})$ represents the intensity of the spatial pattern of appearances around \mathbf{x} , irrespective of the type of pattern. We classify frequent and infrequent appearances by comparing p_0 and q_0 estimated under H_1 after the calculation of $\alpha_A(\mathbf{x})$. Appearances are relatively frequent around \mathbf{x} if

$$p_0 > q_0, \quad (8)$$

while they are infrequent when

$$p_0 < q_0.$$

Frequent and infrequent appearances are denoted by A+ and A-, respectively.

We then visualize the spatial pattern of appearances by using $\alpha_A(\mathbf{x})$. One method is to create a *lattice map*, which visualizes $\alpha_A(\mathbf{x})$ value at lattice points. We distinguish the two types A+ and A- by using different hues as seen in Figure 1. Color saturation indicates the intensity of pattern at each location, while color hue indicates the type of pattern. We should note that our lattice map is different from the grid map mentioned in Section 1. Thicker colors indicate frequent appearances in grid map while they indicate distinctive pattern of appearances in lattice map.

Another method of visualization is to draw circles $Z_0(\mathbf{x}, r)$ that give large $\alpha_A(\mathbf{x})$ as is often done in scan statistics and other statistical methods (Openshaw et al. (1987), Openshaw et al. (1988), Gangnon and Clayton (2001), Conley et al. (2005), Costa and Assunção (2005), Chen et al. (2008), Han et al. (2016)). We draw non-overlapping circles in descending order of $\alpha_A(\mathbf{x})$ until a predetermined number of circles are drawn. The map is called a *circle map* in this paper. Lattice map is effective for grasping the overall picture and regional variation of appearances, while circle map is useful for detecting the regions of distinctive pattern, or more precisely, the regions in which pattern is quite different from that in other regions. Lattice and circle maps are complementary with each other.

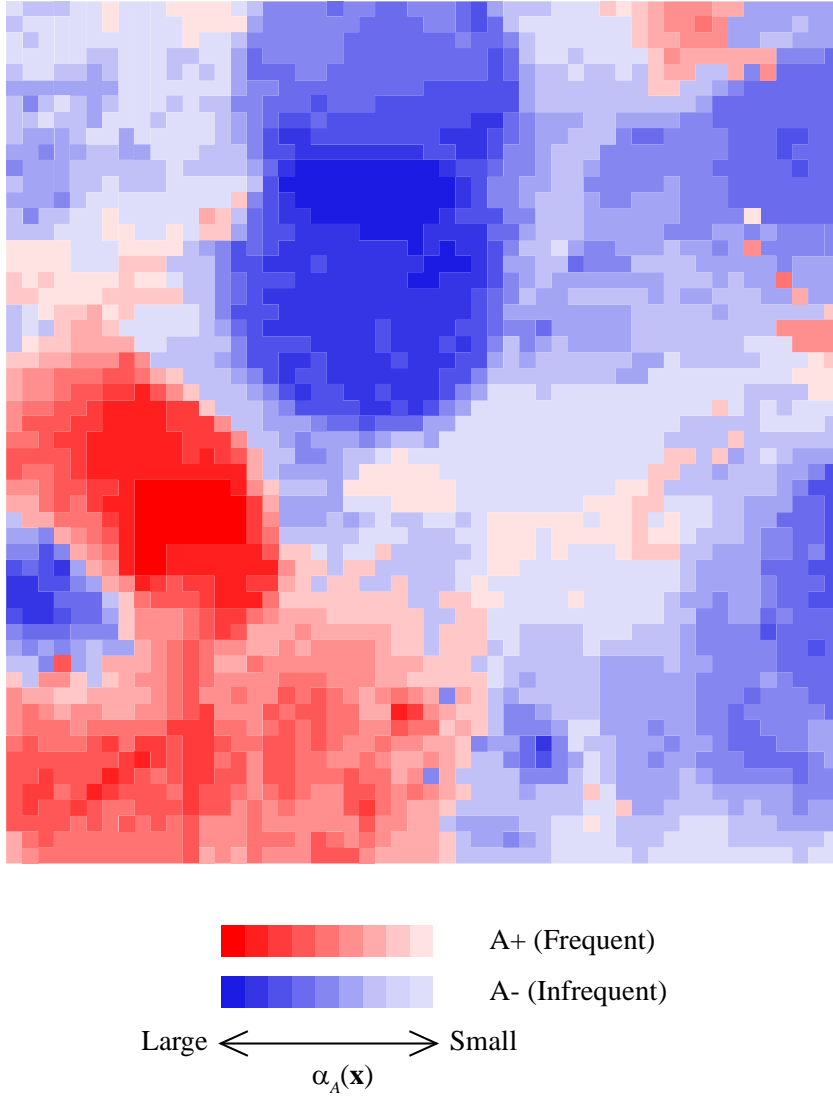


Figure 1 Lattice map of $\alpha_A(\mathbf{x})$. Red and blue shades represent the types of spatial pattern A+ and A-, respectively.

Disappearances are evaluated in a similar manner. Considering disappearances instead of appearances in Equation (6), we calculate the log likelihood ratio $\lambda_D(Z)$. Measure $\alpha_D(\mathbf{x})$ is then given by

$$\alpha_D(\mathbf{x}) = \max_{r \leq r_{\max}} \lambda_D(Q). \quad (10)$$

Pattern of disappearances is classified into two types, i.e., frequent and infrequent disappearances denoted by D+ and D-, respectively.

3.2. Temporal pattern

This subsection considers the temporal pattern of events. We only describe the analysis of appearances since disappearances can be similarly treated. We divide time period T into M sections of equal length $\{T_1, T_2, \dots, T_M\}$. Let Z_i and S_i be the cylinders defined by $Z_0(\mathbf{x}, r) \otimes T_i$ and $S_0 \otimes T_i$, respectively. The probabilities that an appearance occurs in Z_i and $S_i - Z_i$ are denoted by p_i and q_i , respectively. Their sets are represented as $p = \{p_1, p_2, \dots, p_M\}$ and $q = \{q_1, q_2, \dots, q_M\}$. The likelihood function is

$$L^T(Z, p, q) = \prod_i C_{a(Z_i)} p_i^{a(Z_i)} (1 - p_i)^{n(Z_i) - a(Z_i)} C_{a(S_i - Z_i)} q_i^{a(S_i - Z_i)} (1 - q_i)^{n(S_i - Z_i) - a(S_i - Z_i)}. \quad (11)$$

Our interest lies in the temporal pattern of appearances in Z , or more specifically, increase and decrease of appearances in Z . A focus is on the relative change in p and q rather than their absolute values. We thus regard the temporal pattern of appearances is equivalent in Z and $S - Z$ if

$$p_i = k q_i \quad \forall i \in I, \quad (12)$$

where $I = \{1, 2, \dots, M\}$. Equation (12) defines the null hypothesis H_0 . The alternative hypothesis H_1 assumes that temporal pattern of appearances is different between Z and $S - Z$:

$$p_i \neq k q_i \quad \exists i \in I. \quad (13)$$

The likelihood function under H_0 is

$$L^T(Z, k, q) = \prod_i C_{a(Z_i)} k q_i^{a(Z_i)} (1 - k q_i)^{n(Z_i) - a(Z_i)} C_{a(S_i - Z_i)} q_i^{a(S_i - Z_i)} (1 - q_i)^{n(S_i - Z_i) - a(S_i - Z_i)}. \quad (14)$$

It is maximized when

$$\begin{cases} \frac{\partial L^T(Z, k, q)}{\partial q_i} = 0 & (i \in I) \\ \frac{\partial L^T(Z, k, q)}{\partial k} = 0 \end{cases} \quad (15)$$

$$(16)$$

The maximum of $L^T(Z, k, q)$ is denoted as

$$L_0^T(Z) = \max_{p_i = k q_i, \forall i} L^T(Z, p, q). \quad (17)$$

Unfortunately, the simultaneous equations system defined by Equations (15) and (16) is not analytically solvable. We thus derive q_i 's and k numerically by using iterative methods such as the Newton's and Broyden's methods (Ortega and Rheinboldt (1970), Kelley (1995)). Appendix provides initial values of

q_i 's and k that maximize an approximation of the likelihood function $L^T(Z, k, q)$.

The likelihood function maximized under H_1 is given by

$$\begin{aligned} L_1^T(Z) &= \max_{p_i \neq kq_i, \exists i \in I} L^T(Z, p, q) \\ &= \prod_i n(Z_i) C_{a(Z_i)} \left(\frac{a(Z_i)}{n(Z_i)} \right)^{a(Z_i)} \left(1 - \frac{a(Z_i)}{n(Z_i)} \right)^{n(Z)-a(Z_i)} \\ &\quad n(S_i-Z_i) C_{a(S_i-Z_i)} \left(\frac{a(S_i-Z_i)}{n(S_i-Z_i)} \right)^{a(S_i-Z_i)} \left(1 - \frac{a(S_i-Z_i)}{n(S_i-Z_i)} \right)^{n(S_i-Z_i)-a(S_i-Z_i)}. \end{aligned} \quad (18)$$

The log likelihood ratio is

$$\lambda_A^T(Z) = \log L_1^T(Z) - \log L_0^T(Z). \quad (19)$$

We maximize $\lambda_A^T(Z)$ by expanding circle $Z_0(\mathbf{x}, r)$ from a small one until its radius reaches at a predetermined length r_{\max} . The maximum value $\alpha_A^T(\mathbf{x})$ (and $\alpha_D^T(\mathbf{x})$ for disappearances) is given by

$$\alpha_A^T(\mathbf{x}) = \max_{r \leq r_{\max}} \lambda_A^T(Z). \quad (20)$$

Measure $\alpha_A^T(\mathbf{x})$ represents the intensity of the temporal pattern of appearances at \mathbf{x} . Similar to $\alpha_A(\mathbf{x})$, $\alpha_A^T(\mathbf{x})$ does not indicate the property of temporal pattern, i.e., it is unknown how the pattern is different in Z from that in $S-Z$. To evaluate the difference, we define k_i and its standardized form κ_i as

$$k_i = \frac{P_i}{q_i} \quad (21)$$

and

$$\kappa_i = \frac{k_i}{\frac{1}{M} \sum_i k_i}, \quad (22)$$

respectively. If $\kappa_i > 1$, appearances in Z_i is relatively more frequent than those in S_i-Z_i , while appearances are less frequent when $\kappa_i < 1$. Comparing each κ_i with 1, we can grasp the temporal pattern of appearances in Z . When $M=2$, for instance, we will find one of the following two cases:

$$\kappa_1 < 1, \kappa_2 > 1 \quad (23)$$

or

$$\kappa_1 > 1, \kappa_2 < 1 \quad (24)$$

The former indicates that appearances in Z increased more than those in $S-Z$ from T_1 to T_2 , while the latter

means the relative decrease of appearances. We denote the two cases A_I and A_D (and D_I and D_D for disappearances), respectively.

The number of possible cases is 2^{M-1} . It increases rapidly with M , which makes their interpretation more complicated. When M is large, therefore, it is effective to summarize the set $\{\kappa_1, \kappa_2, \dots, \kappa_M\}$ into a single measure. Spearman's rank correlation coefficient ρ of κ_i is useful for representing the monotonicity of temporal pattern. If appearances increase in Z , κ_i increases with i , and ρ shows a large value. Decrease of appearances, on the other hand, yields a negative ρ value. Variance and statistics used in runs test can describe the fluctuation and randomness of κ_i . The maximum of κ_i can be used for detecting temporal outliers.

Visualization method of $\alpha_A^T(\mathbf{x})$ also depends on M . If $M=2$, temporal pattern can be visualized by both lattice and circle maps. If $M>2$, lattice map is effective for visualizing the spatial distribution of the summary measures of κ_i 's.

3.3. Multiple patterns

So far we have considered the spatial and temporal patterns of appearances and disappearances. Each pattern is classified into two types, i.e., $\{A+, A-\}$, $\{D+, D-\}$, $\{A_I, A_D\}$, and $\{D_I, D_D\}$, all of which are visualized as separate maps. This subsection, on the other hand, considers the visualization of multiple patterns in a single map. This aims to help the understanding of the relationship between different patterns such as the spatial patterns of appearances and disappearances. Suppose there are K patterns. Let $\lambda_j(Z(\mathbf{x}, r))$ and $\alpha_j(\mathbf{x})$ be the log likelihood ratio of pattern j in cylinder Z and its maximum value, respectively.

When K is small, a simple but effective method is to overlay lattice maps of different patterns. Suppose the spatial patterns of appearances and disappearances. We assign pattern types $A+$, $A-$, $D+$, and $D-$ four different hues such as red, yellow, cyan, and blue. Using these color hues, we generate and overlay two lattice maps that indicate the spatial pattern of appearances and disappearances. This permits us to understand the spatial relationship between appearances and disappearances. When $4 \leq K$, overlay of lattice maps is not effective. Patterns need to be visualized as separate maps each of which indicates one or two patterns.

Circle map is also useful to visualize multiple patterns. Overlay of circle maps, however, often causes circle overlap, which makes the map too complicated for visual exploration. To avoid this problem, we summarize $\lambda_j(Z(\mathbf{x}, r))$'s into a single measure by which we can draw circles in a single map without overlap. A primary objective of circle map is to indicate the regions where patterns are quite different from other regions. Summary measure thus needs to indicate the overall intensity of multiple patterns. One method is to sum up all the $\lambda_j(Z(\mathbf{x}, r))$'s as is done in multivariate scan statistic:

$$\lambda(Z(\mathbf{x}, r)) = \sum_j \lambda_j(Z(\mathbf{x}, r)) \quad (25)$$

(Kulldorff et al. 2007). Maximizing $\lambda(Z(\mathbf{x}, r))$, we obtain

$$\alpha(\mathbf{x}) = \max_{r \leq r_{\max}} \lambda(Z(\mathbf{x}, r)). \quad (26)$$

We draw non-overlapping circles according to $\alpha(\mathbf{x})$ in descending order. This method, however, extracts both the regions where all the patterns are relatively distinctive and those where only a single pattern is extremely distinctive. The latter are detectable by evaluating individual patterns separately, which does not meet the objective of treating multiple patterns simultaneously. We thus propose another summary measure to find the locations where all the patterns are relatively distinctive. Let $\delta_j(\mathbf{x}, r_0, r)$ be a binary function defined as

$$\delta_j(\mathbf{x}, r_0, r) = \begin{cases} 1 & \text{if } \lambda_j(Z(\mathbf{x}, r_0)) \leq \lambda_j(Z(\mathbf{x}, r)) \\ 0 & \text{otherwise} \end{cases} \quad (27)$$

Rank function $R_j(Z(\mathbf{x}, r))$ is defined by

$$R_j(Z(\mathbf{x}, r)) = \frac{1}{r_{\max}} \int_{r_0 \leq r_{\max}} \delta_j(\mathbf{x}, r_0, r) dr_0 \quad (28)$$

This function shows the relative rank of $\lambda_j(Z(\mathbf{x}, r))$ in $r \in [0, r_{\max}]$, ranging from zero to one. It becomes large if $\lambda_j(Z(\mathbf{x}, r))$ is relatively large in $r \in [0, r_{\max}]$. Using $R_j(\mathbf{x}, r)$, we define

$$R_{\min}(\mathbf{x}, r) = \min_{j \in \{1, \dots, K\}} R_j(\mathbf{x}, r). \quad (29)$$

This indicates the rank of the least distinctive pattern among K patterns in $Z(\mathbf{x}, r)$. Using this function, we determine radius r where the rank of the least distinctive pattern is the highest in $[0, r_{\max}]$:

$$R_{\max}(\mathbf{x}) = \max_{r \leq r_{\max}} R_{\min}(\mathbf{x}, r). \quad (30)$$

This procedure permits us to detect the regions where all the patterns are relatively distinctive, in other words, any pattern is not indistinctive. The log likelihood ratio at \mathbf{x} is given by

$$\alpha'(\mathbf{x}) = \sum_j \lambda_j(Z(\mathbf{x}, r_{\max})), \quad (31)$$

where r_{\max} is the value of r that maximizes $R_{\min}(\mathbf{x}, r)$. We draw circles following $\alpha'(\mathbf{x})$ in descending order without overlap until a predetermined number of circles are drawn.

4. Application to real data

This section tests the performance of the method proposed in the previous section. We analyze the distribution of retail stores and restaurants in Shibuya-ku, Tokyo, Japan, from 2001 to 2016. The NTT TownPage cooperation provides the telephone directory of commercial facilities in Japan. We converted the list into spatial data by geocoding. Figure 2 shows the study region, where residential area spreads along Keio and Odakyu Lines. One of the largest commercial areas in Tokyo expands around Shibuya, Harajuku, and Omotesando stations. Smaller ones also exist around Yoyogi, Daikan-yama, and Ebisu stations. Small shopping malls are found around the stations of Keio and Odakyu Lines.

We calculated the proposed measures for ten different categories of stores by using a program written in C++. Lattice map consisted of 100 by 100 lattice points, while circle map contained ten circles in the study area. We set r_{\max} to 500 meters, and gradually increased the radius r from 10 by 10 meters. Calculation of $\alpha^T_A(\mathbf{x})$ and $\alpha^T_D(\mathbf{x})$ utilized Newton-Rhapson and quasi Newton methods. The processing time on a i7-7500U, CPU 2.70GHz, RAM 32GB computer was approximately one minute for each category. We will show the result of analysis of clothing stores, restaurants, and clinics due to space limitation in the following. The numbers of these facilities that existed at least once from 2001 to 2016 in the study region are 9510, 12685, and 3261, respectively. Figures 3, 4, and 5 show their distribution in 2016 represented by kernel density functions.

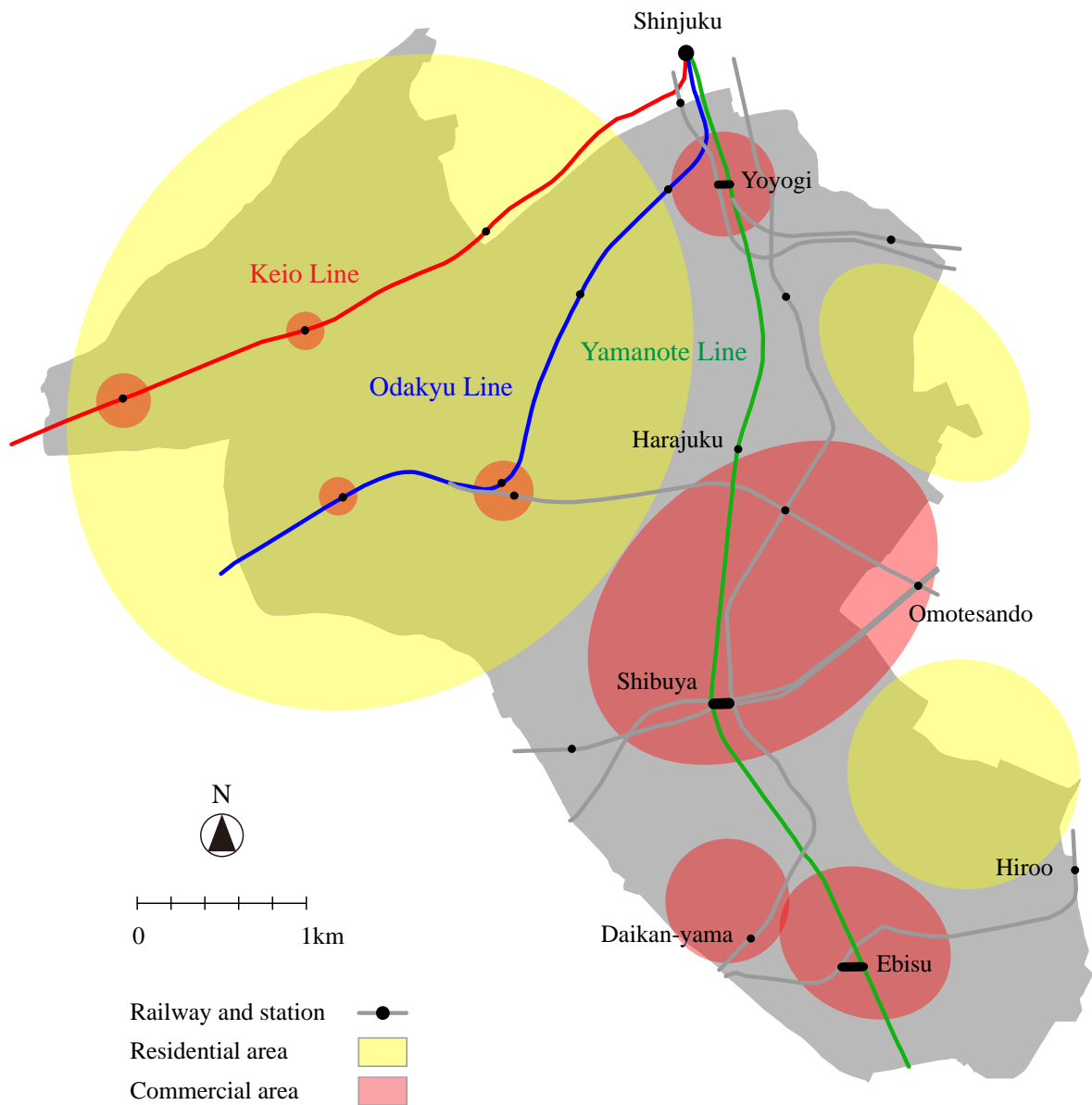


Figure 2 Study region: Shibuya-ku, Tokyo, Japan.

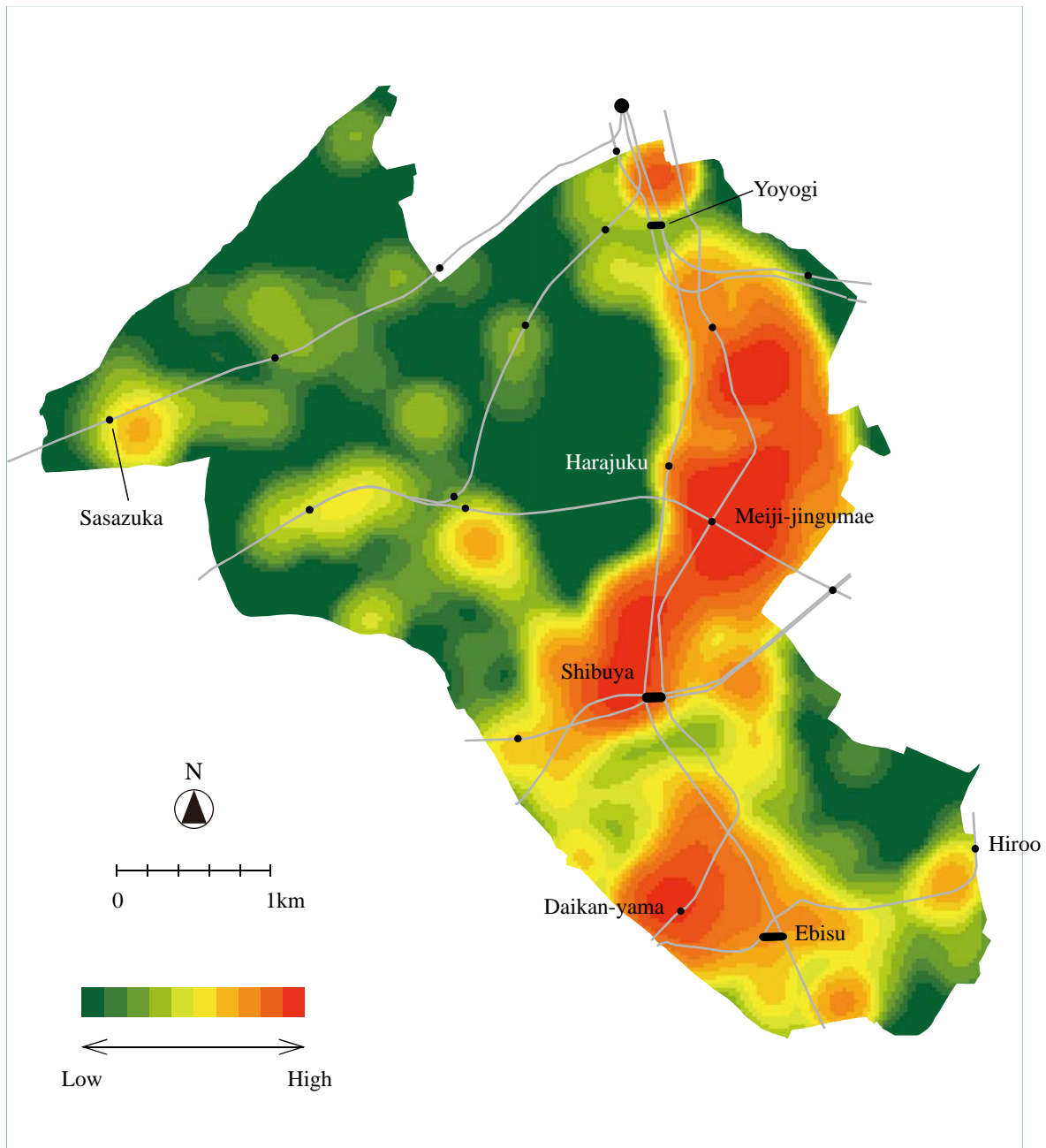


Figure 3 Distribution of clothing stores represented by the kernel density function in 2016 in Shibuya-ku, Tokyo, Japan.

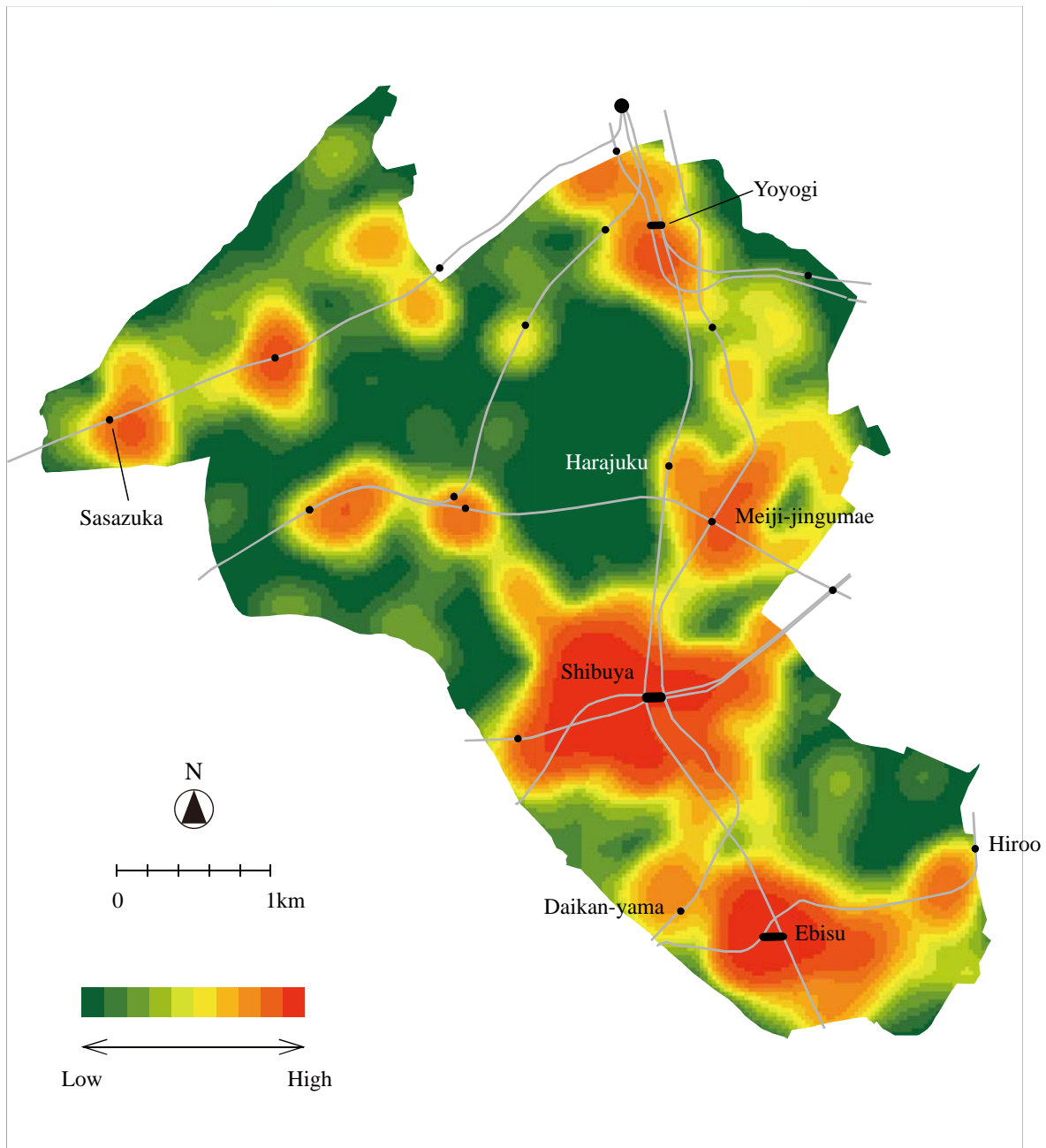


Figure 4 Distribution of restaurants represented by the kernel density function in 2016 in Shibuya-ku, Tokyo, Japan.

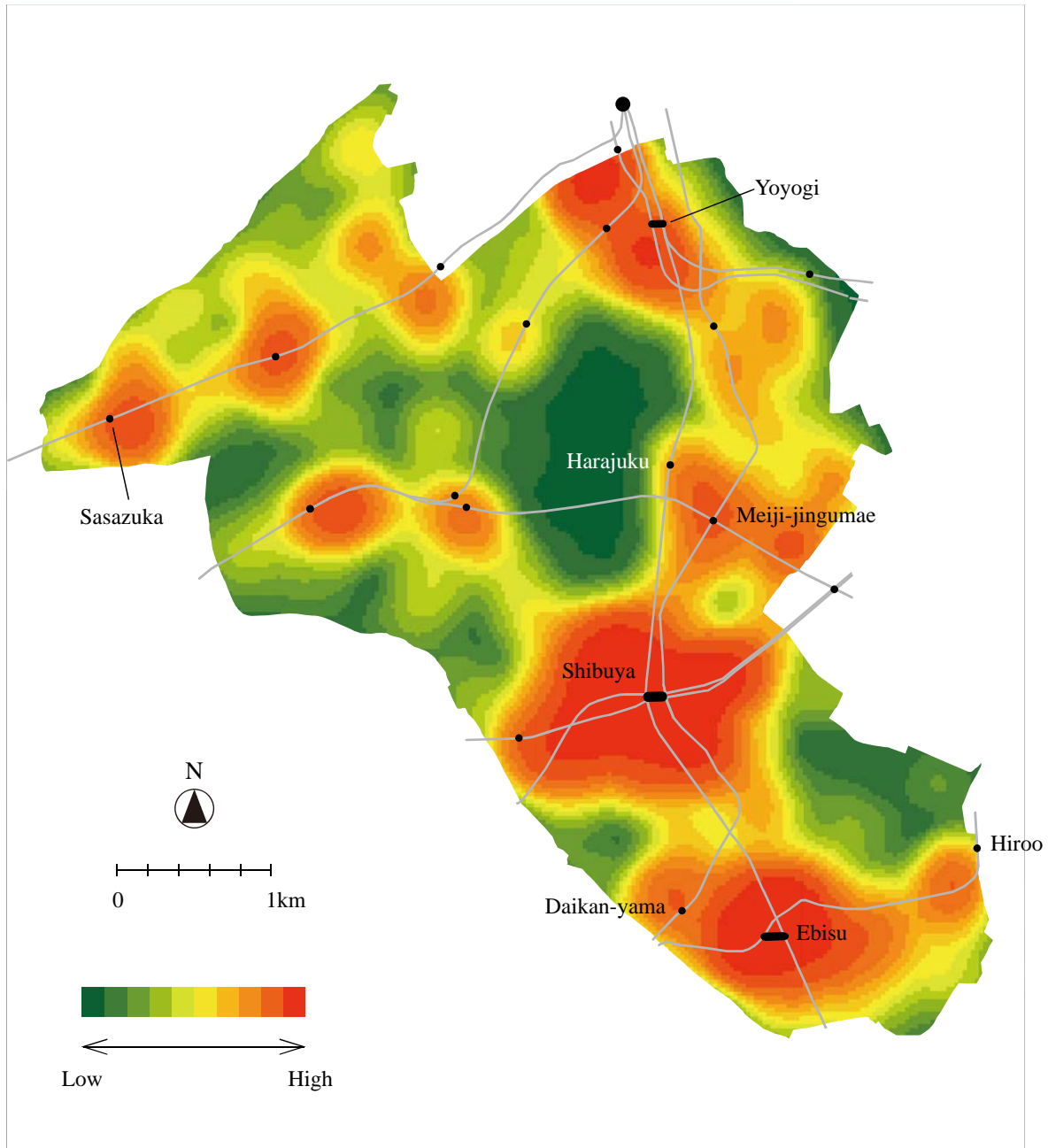


Figure 5 Distribution of clinics represented by the kernel density function in 2016 in Shibuya-ku, Tokyo, Japan.

4.1 Spatial pattern of openings and closures

This subsection considers the spatial patterns of openings and closures of stores. We treat the two patterns simultaneously by using the method proposed in Subsection 3.3. Red, cyan, blue, and yellow represent A+, A-, D+, and D-, respectively.

Figure 6 shows the lattice map of clothing stores. Thick purple indicates frequent openings and closures, which implies a competitive and active commercial environment. Thick green observed around Sasazuka, Shibuya & Ebisu stations represents infrequent openings and closures, where competition is not so severe. The figure almost corresponds to Figure 3, i.e., stores change frequently where stores are densely located while stores do not change where stores are sparse. Exceptions include the areas around Sangubashi station and the east of Ebisu station where openings and closures are frequent though stores are rather sparse.

Figure 7 shows the lattice map of restaurants. Unlike Figure 6, Figure 7 is not similar to the distribution of restaurants shown in Figure 4. Differences are observed around Yoyogi, Shibuya, and Ebisu stations. Openings and closures are not frequent around Yoyogi and Shibuya stations though restaurants are densely located. The latter is due to the cluster of traditional restaurants close to Shibuya station that have been supported a long time by loyal customers. Openings are frequent while closures are infrequent around Ebisu station. Restaurants have increased due to a rapid expansion of commercial area to the west.

Figure 8 is the lattice map of clinics. The figure is partially similar to the distribution of clinics shown in Figure 5, where clinics are generally clustered around railway stations. Openings and closures are frequent around Harajuku, Shibuya, and Ebisu stations of Yamanote Line while they are not frequent around Keio Line stations. This occurs due to the difference in the accessibility to the stations. Stations of Yamanote Line are accessible by multiple railway lines and hence have a wider market area than Keio Line stations. Competition is keen around the former stations, which leads to frequent openings and closures.

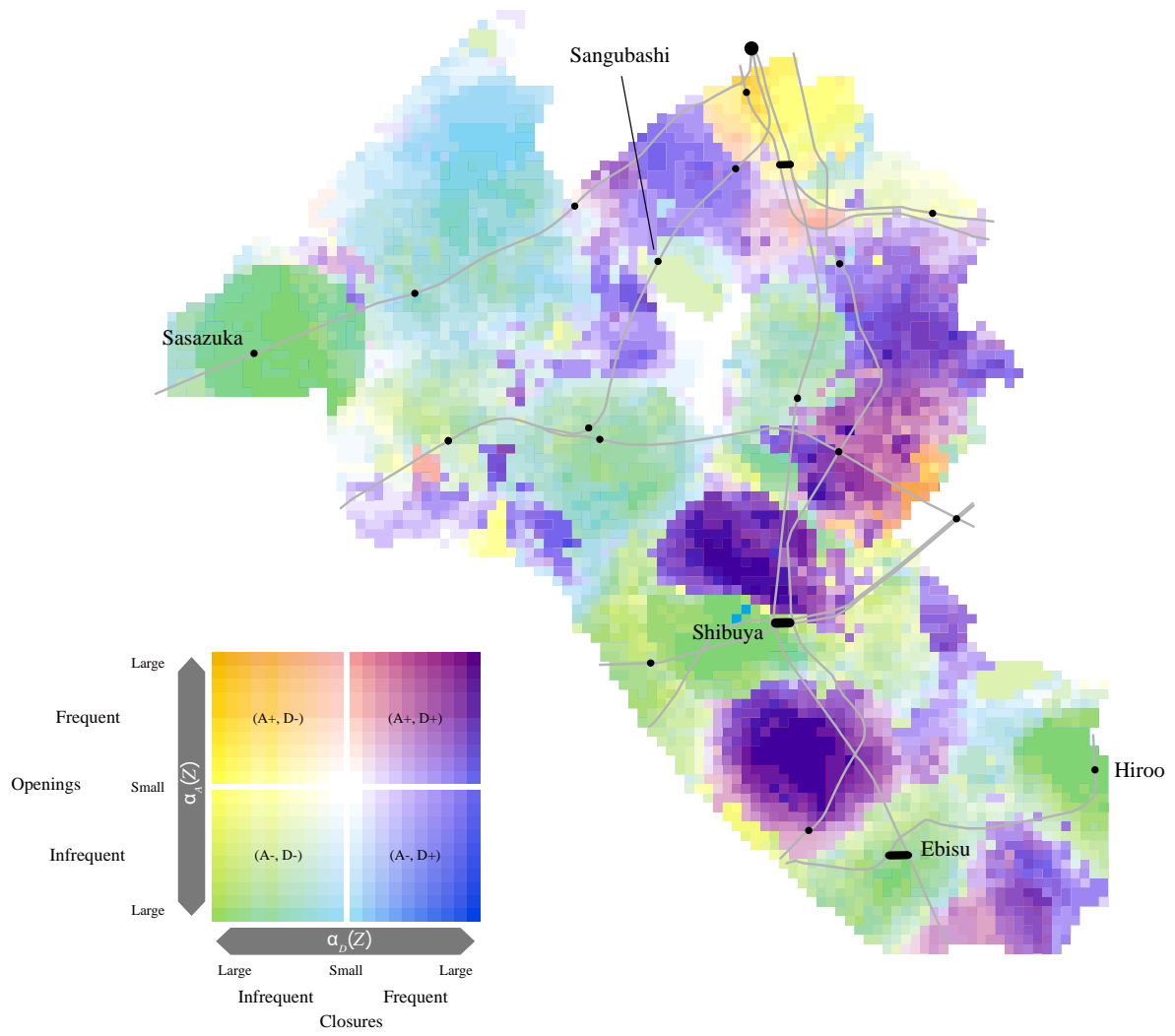


Figure 6 Lattice map of $\alpha_A(Z)$ and $\alpha_D(Z)$ of clothing stores.

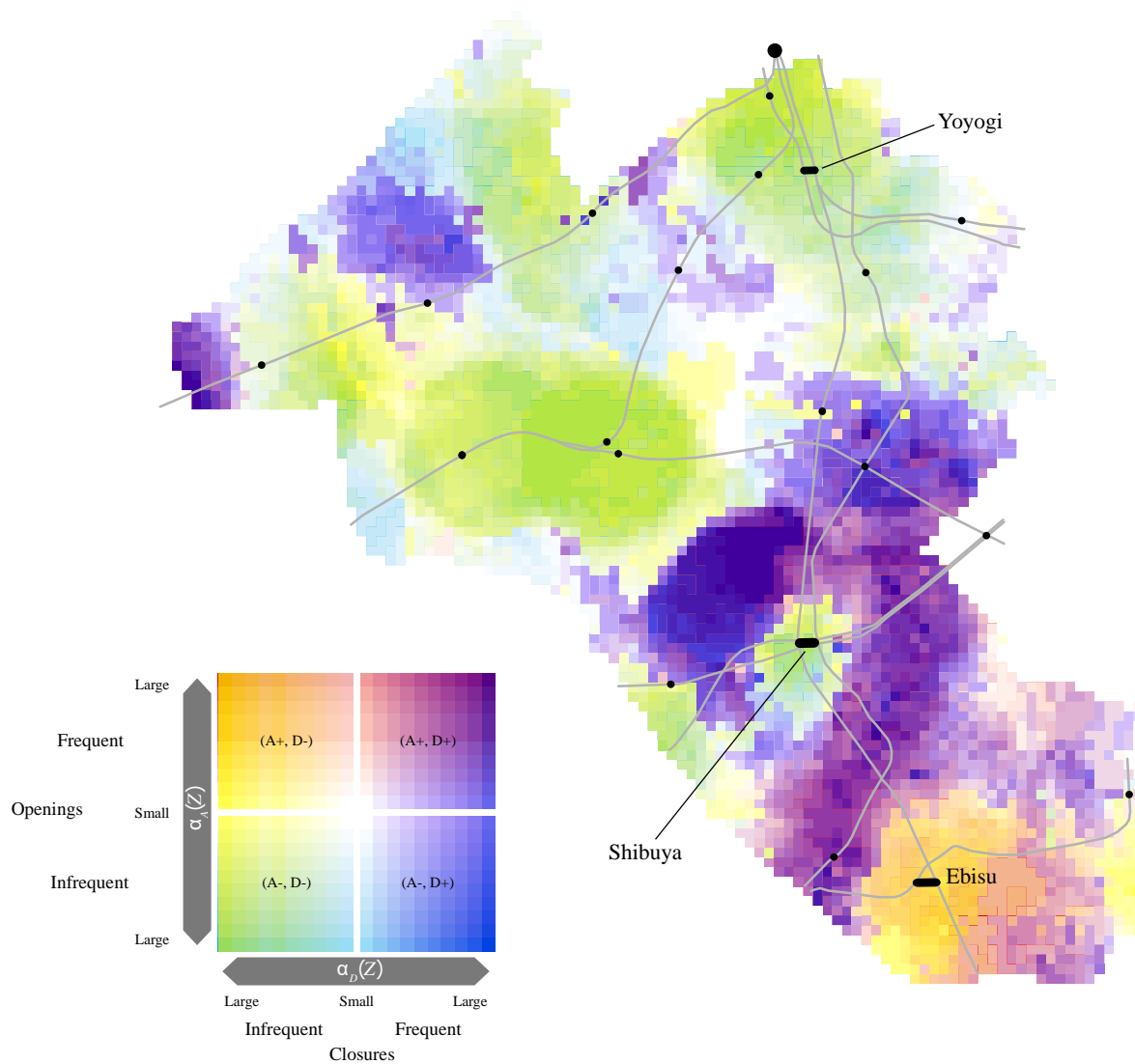


Figure 7 Lattice map of $\alpha_A(Z)$ and $\alpha_D(Z)$ of restaurants.

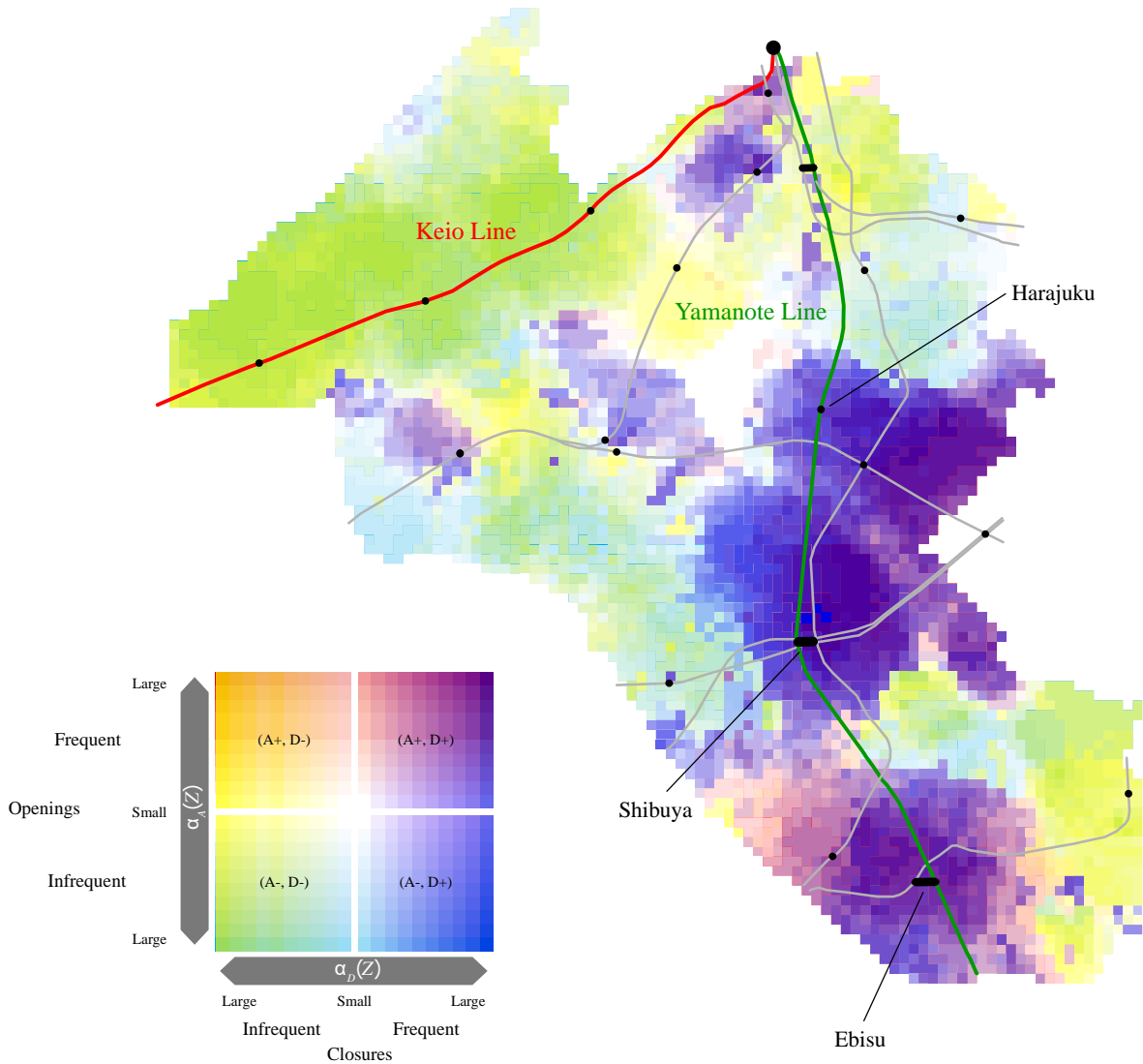


Figure 8 Lattice map of $\alpha_A(Z)$ and $\alpha_D(Z)$ of clinics.

Figures 9 and 10 show the circle maps of clothing stores and restaurants. The figures almost correspond to Figures 6 and 7, i.e., circles are located in the regions of thicker colors in lattice maps. A strength of circle map is that it indicates the intensity of patterns more clearly than lattice map. For instance, neighborhoods of Sasazuka, Shibuya, Ebisu, and Hiroo stations look quite similar in Figure 6. Figure 9 clearly distinguishes these regions, i.e., circles in the west of Shibuya station are ranked 1st and 3rd and hence more distinctive than those around Hiroo and Sasazuka stations ranked 5th and 6th. Circle map, on the other hand, does not show the spatial variation of pattern inside circles. The periphery of the 5th circle in Figure 9 is indicated by blue shades in Figure 6, which implies that closures are not infrequent. Similarly, a spatial variation exists in the pattern in the 9th circle in Figure 10.

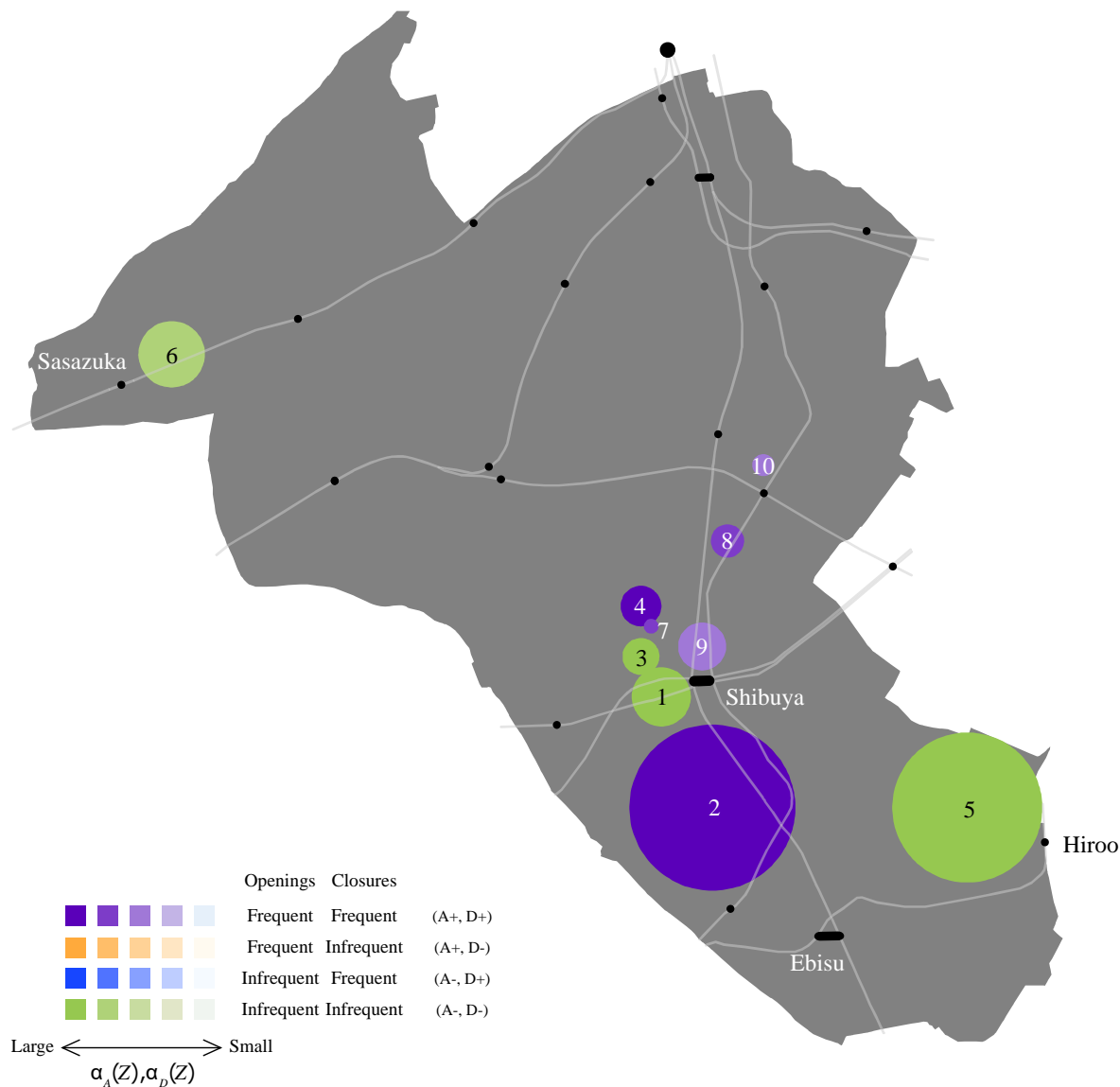


Figure 9 Circle map of spatial pattern of clothing stores. Numbers indicate the rank of circles evaluated by $\alpha(\mathbf{x})$.

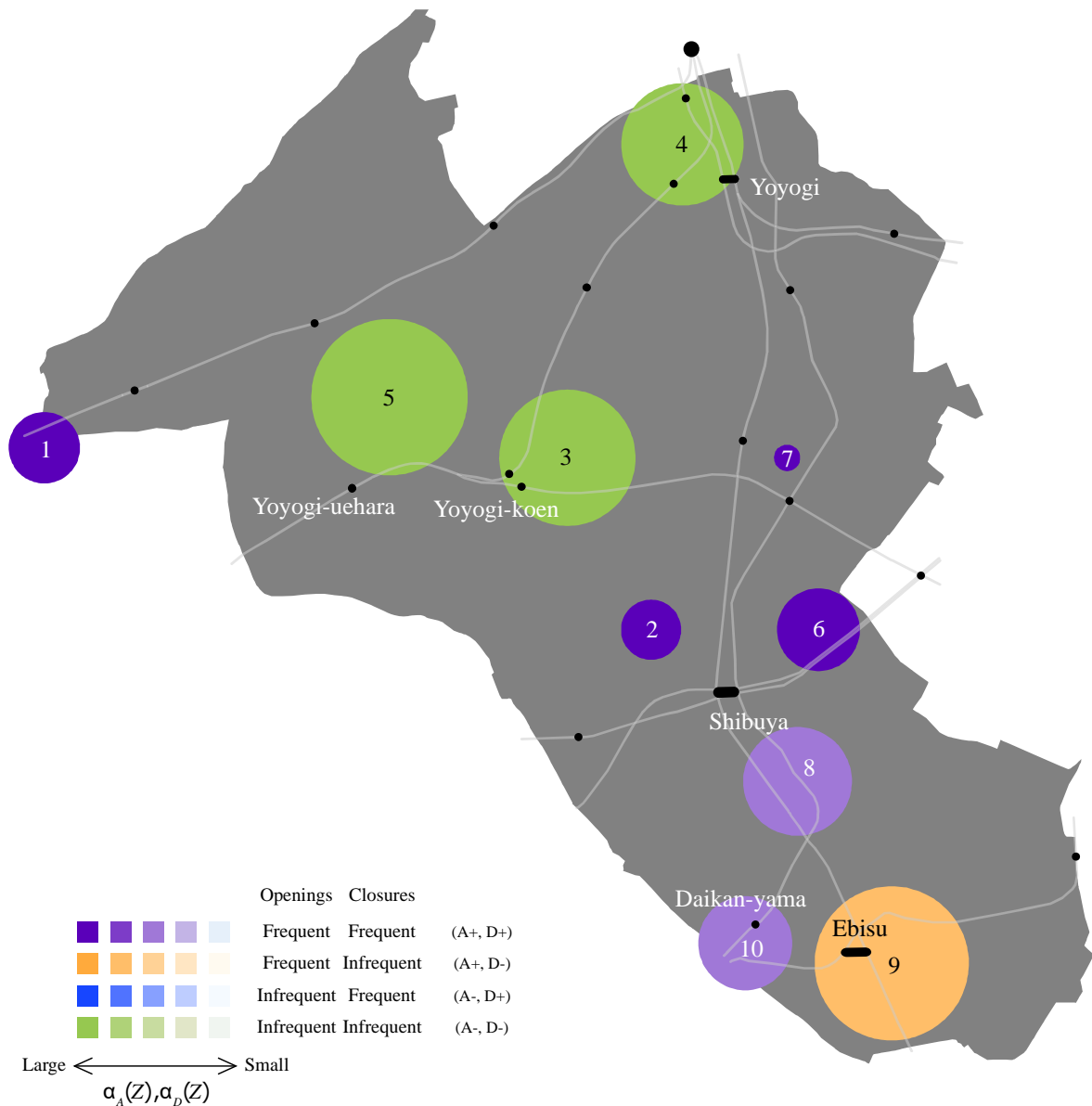


Figure 10 Circle map of spatial pattern of restaurants. Numbers indicate the rank of circles evaluated by $\alpha(\mathbf{x})$.

4.2 Temporal pattern of openings and closures

This subsection analyzes the temporal pattern of openings and closures. We first set M to 2 to use both lattice and circle maps. The whole period is divided into two sections 2001-08 and 2009-16, which are denoted by T_1 and T_2 , respectively. Lattice map utilizes red, cyan, blue, and yellow to represent A_I , A_D , D_I , and D_D , respectively.

Figure 11 shows the lattice maps of $\alpha_A^T(Z)$ and $\alpha_D^T(Z)$ of clothing stores overlaid into a single map. Thick blue in the north of Shibuya station indicates the decrease of openings and the increase of

closures from T_1 to T_2 . This suggests the decline of clothing stores in this area. Light green in the north of Daikan-yama station indicates the decrease of openings and closures, where frequent openings and closures are observed in Figure 6. This implies that the competition between clothing stores had become less fierce from T_1 to T_2 . Orange shades in the west of Yoyogi station show an increase of openings and a decrease of closings. Considering the frequent openings in this area reported in Figure 6, we may expect a fierce competition in the near future in this area.

Figure 12 shows the lattice map of restaurants. Light green in the north of Shibuya station indicates the decrease of openings and closures. This implies that the competition supposed in Figure 7 had decreased from T_1 to T_2 . Orange shades around Meiji-jingumae station represent an increase of openings and a decrease of closures. This suggests the growth of the cluster of restaurants shown in Figure 4.

Figure 13 is the lattice map of clinics. Thick purple around Yoyogi-uehara and Ebisu stations, and the north of Omotesando station indicates an increase of openings and closures of clinics. Orange shades in the north of Yoyogi-koen station and the south of Yoyogi station represent an increase of openings and decrease of closures. Both color shades are located in residential areas and suggest an increase of competition from T_1 to T_2 .

Figures 11-13 show more regional variation than Figures 6-8. A primary reason is that temporal analysis treats fewer events in each cylinder $Z_i(\mathbf{x}, r)$ than those in $Z(\mathbf{x}, r)$ in spatial analysis. Measures $\alpha_A^T(\mathbf{x})$ and $\alpha_D^T(\mathbf{x})$ are fluctuated than $\alpha_A(\mathbf{x})$ and $\alpha_D(\mathbf{x})$, which increases their regional variation. Figure 13 looks more complicated than Figures 11 and 12 because clinics are fewer than clothing stores and restaurants.

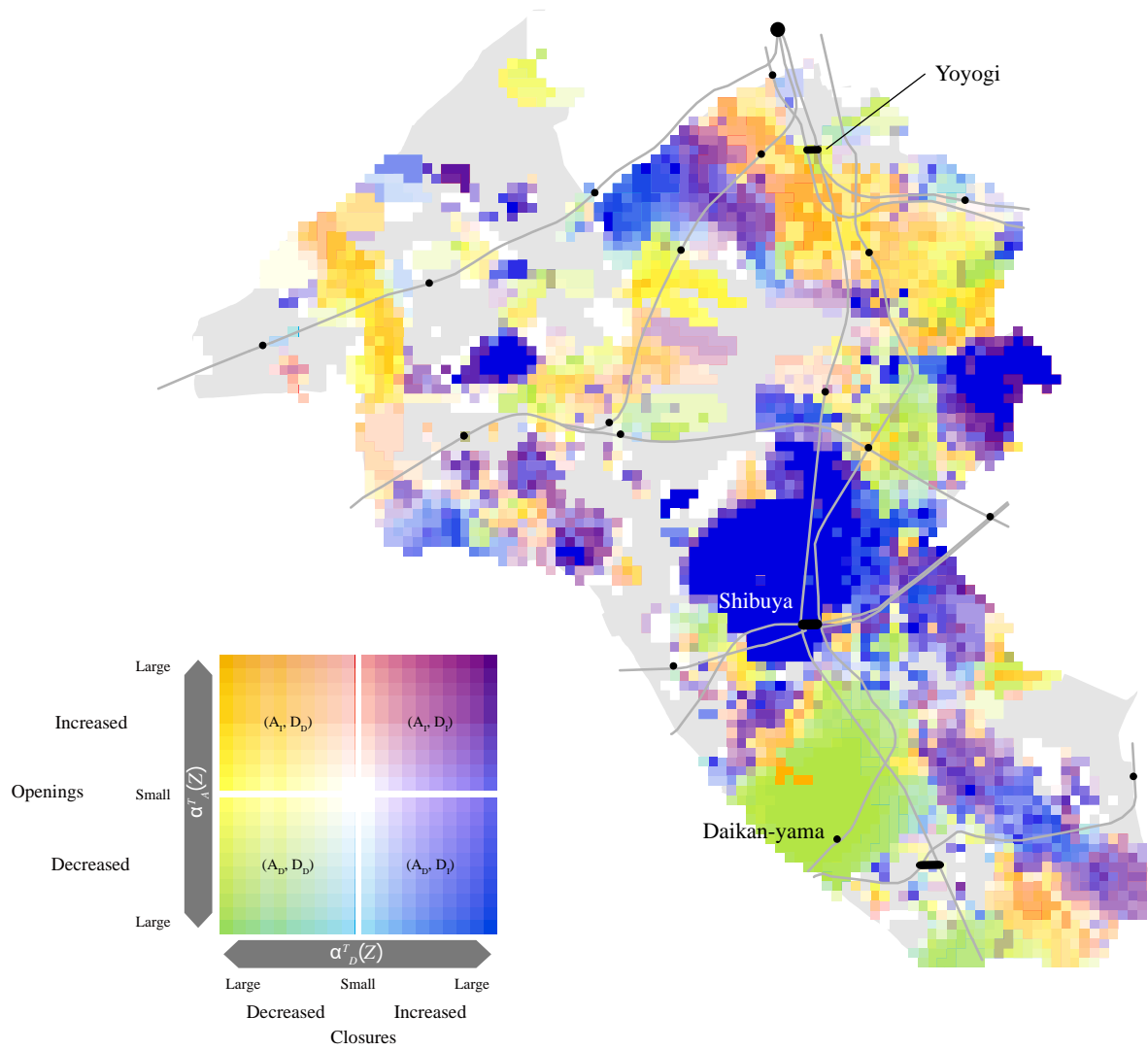


Figure 11 Lattice map of $\alpha_A^I(Z)$ and $\alpha_D^I(Z)$ of clothing stores.

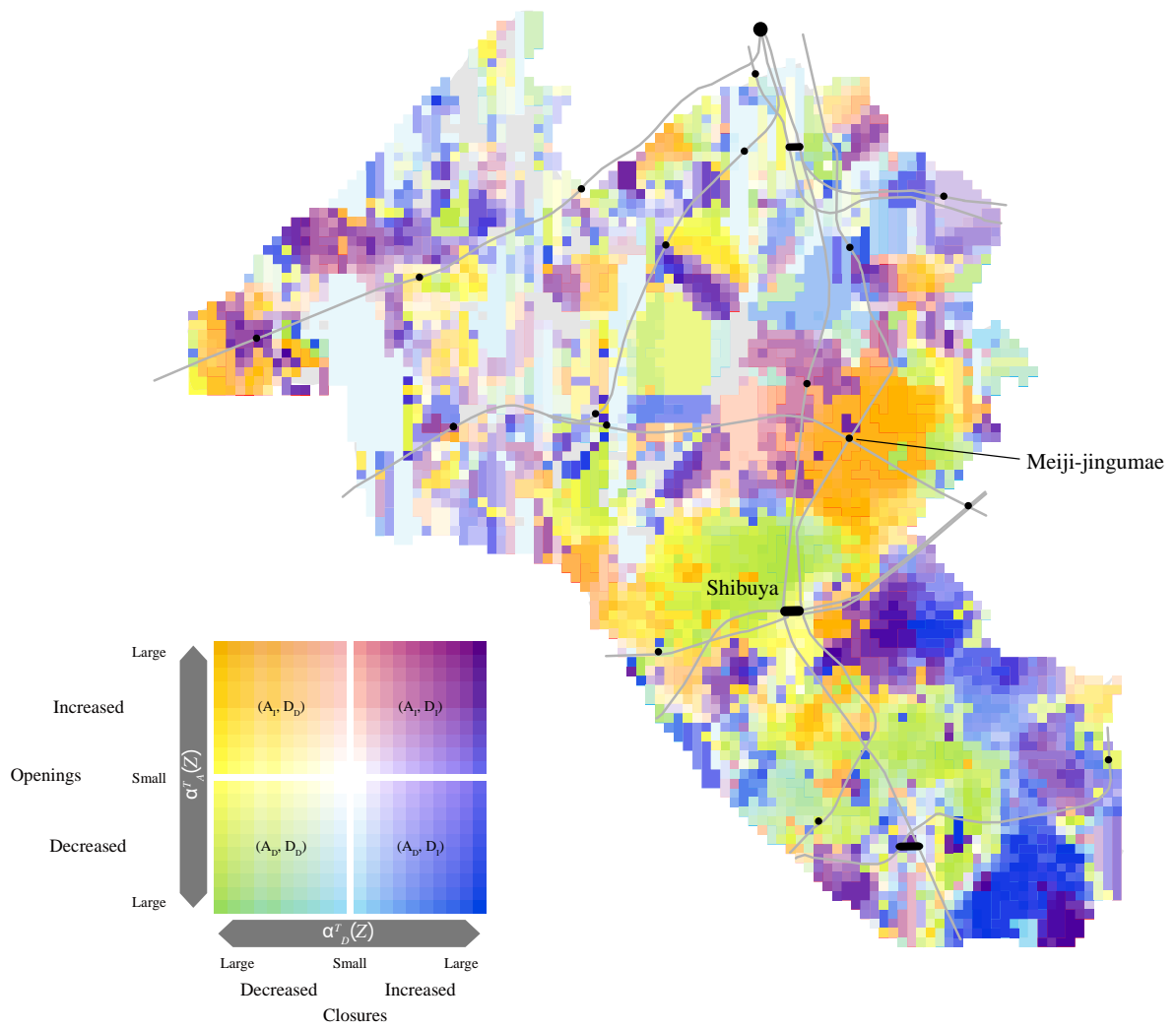


Figure 12 Lattice map of $\alpha_A^T(Z)$ and $\alpha_D^T(Z)$ of restaurants.

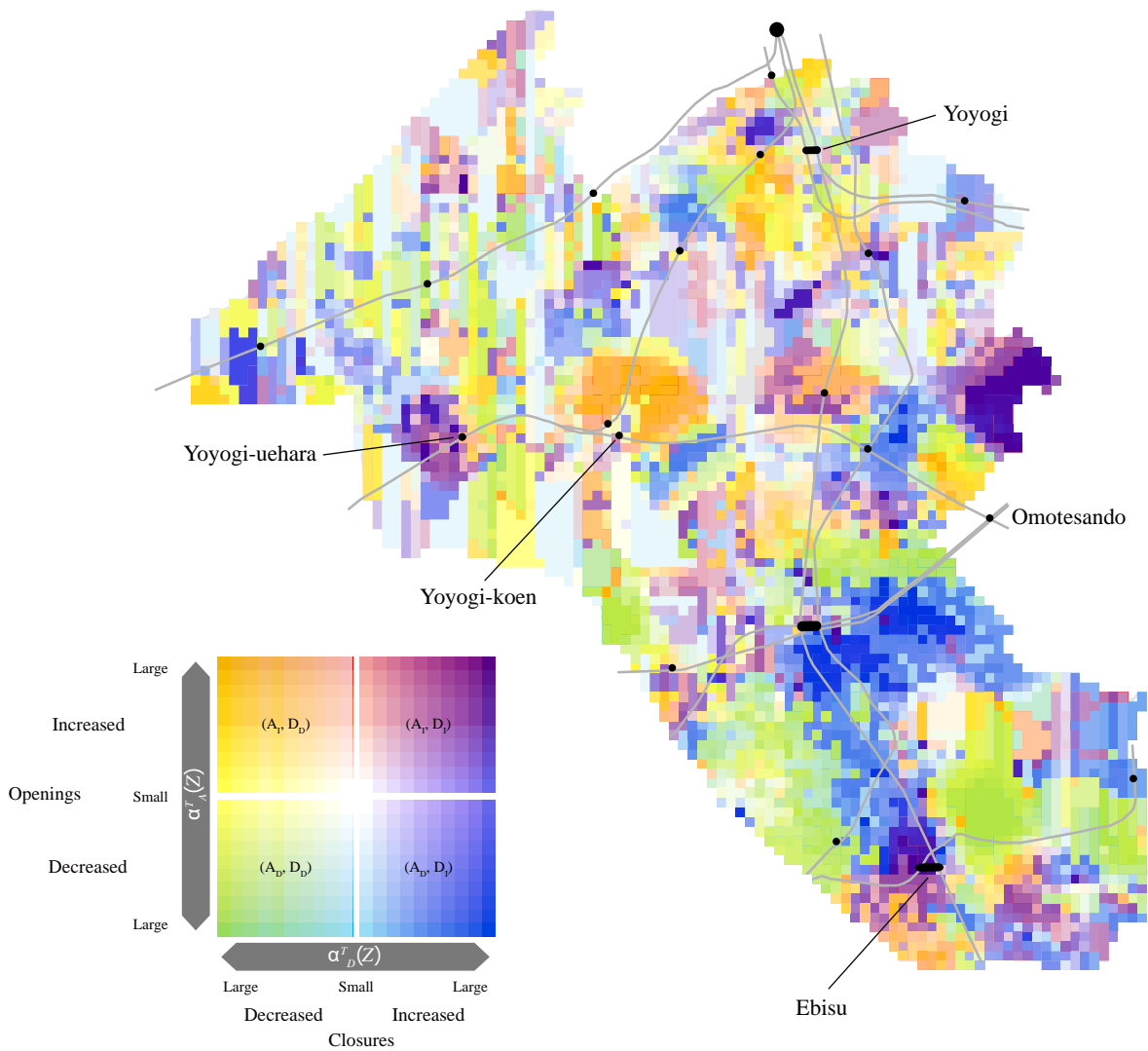


Figure 13 Lattice map of $\alpha_A^T(Z)$ and $\alpha_D^T(Z)$ of clinics.

Figures 14 and 15 show the circle maps of clothing stores and restaurants, respectively. Similar to the circle maps of spatial pattern, these figures correspond well with lattice maps shown in Figures 11 and 12. Examples include the 1st, 2nd, and 4th circles in Figure 14 and the 1st, 2nd, and 3rd circles in Figure 15. Circle map is effective especially when lattice map looks complicated as seen in Figures 11-13. Figure 14, for instance, indicates small but distinctive circles such as the 2nd, 3rd, and 5th circles that are not easily detectable in Figure 11. The 4th, 5th and 6th circles in Figure 15 are also difficult to find in Figure 12.

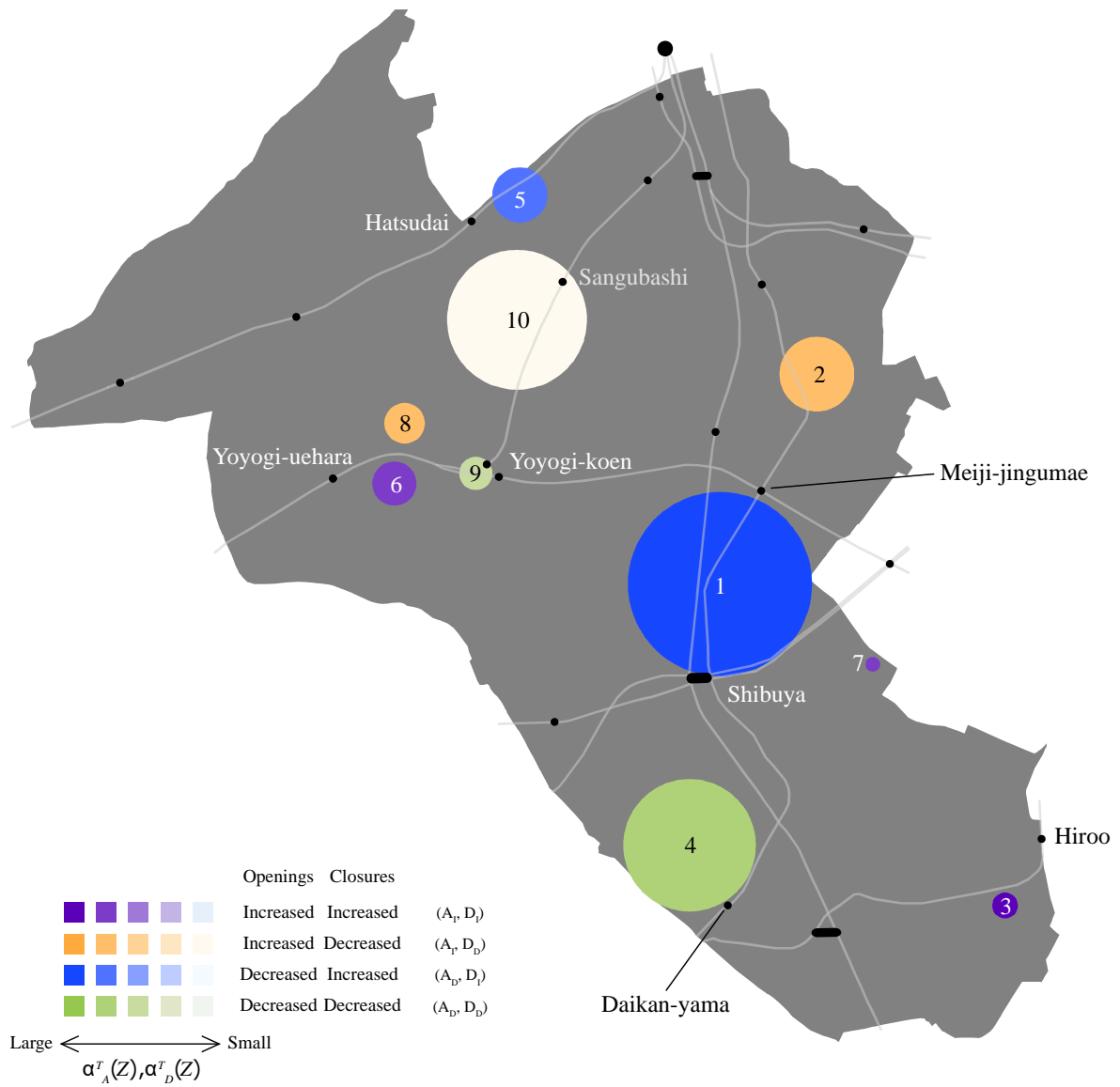


Figure 14 Circle map of the temporal pattern of clothing stores. Numbers indicate the rank of circles evaluated by $\alpha^T(\mathbf{x})$.

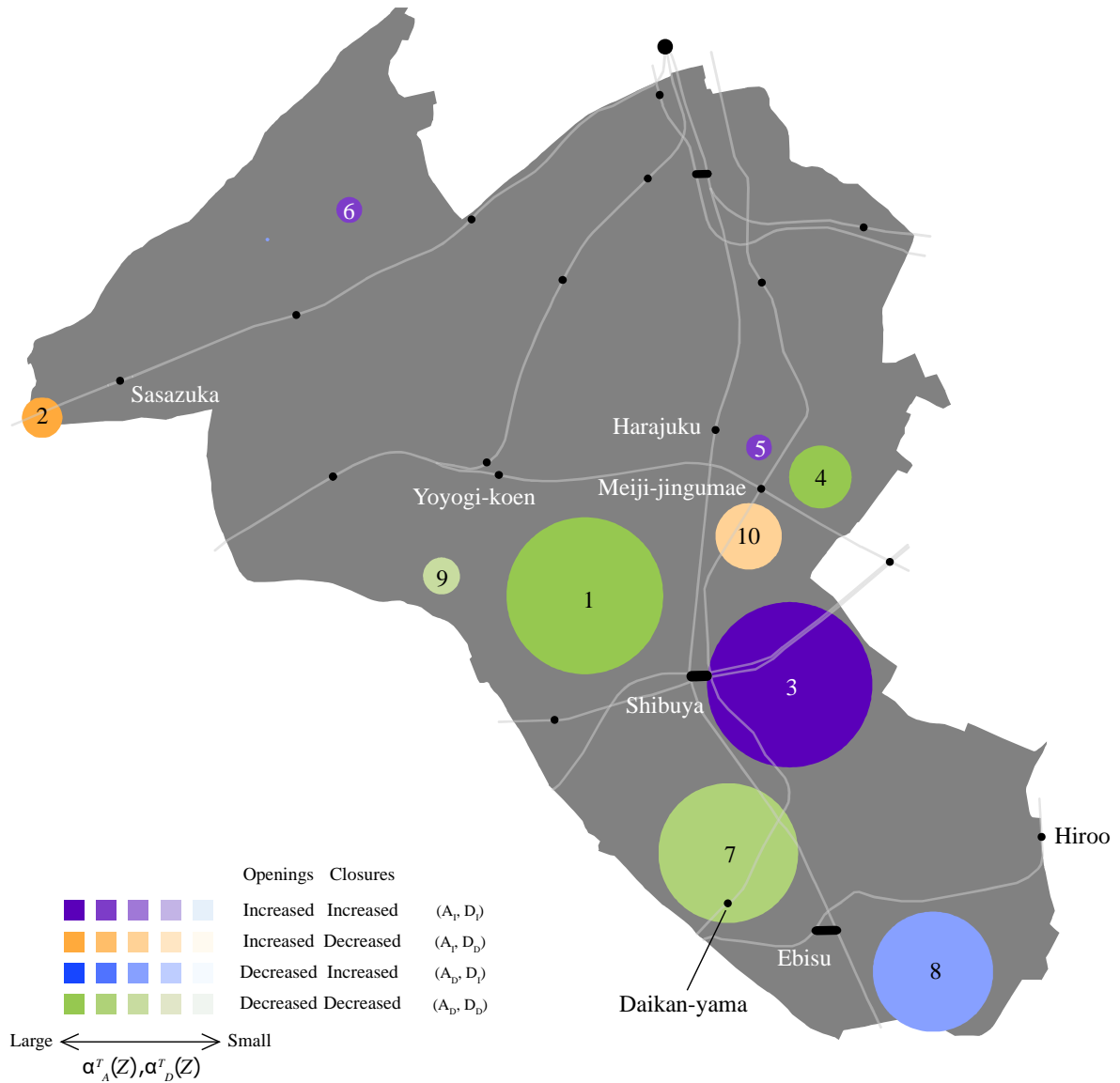


Figure 15 Circle map of the temporal pattern of restaurants. Numbers indicate the rank of circles evaluated by $\alpha^T(\mathbf{x})$.

We finally set M to 8, i.e., the whole period is divided into eight sections to evaluate the temporal pattern of openings and closures in more detail. Spearman's rank correlation coefficient ρ of κ_i is visualized as lattice maps. Figure 16 shows the lattice map of the openings of clothing stores. Thick red around Yoyogi station indicates that store openings almost monotonically increased in this area. This is consistent with orange shades around Yoyogi station in Figure 11. Thick green around Daikan-yama station indicates a constant decrease of openings, which also corresponds to the light green in the same area in Figure 11. Thick blue in the west of Shibuya station in Figure 11 is represented as a mixture of different colors in Figure 16. Regional variation exists in the temporal pattern of openings in this area,

which is not shown in Figure 11. Figure 17 shows the lattice map of the openings of restaurants. The figure reveals a steady increase of openings around Meiji-jingumae station, which corresponds to the orange shades in Figure 12. Decrease of openings in the north of Shibuya station in Figure 12 is found to vary among locations in Figure 17. Figures 18 and 19 shows the maps of closures of clothing stores and restaurants, respectively. Figure 18 shows that closures monotonically decreased around Daikan-yama station, which cannot be known in Figure 11. Figure 19 indicates a steady increase of closures in the east of Shibuya station and the west of Hiroo station, which is rather vague in Figure 12.

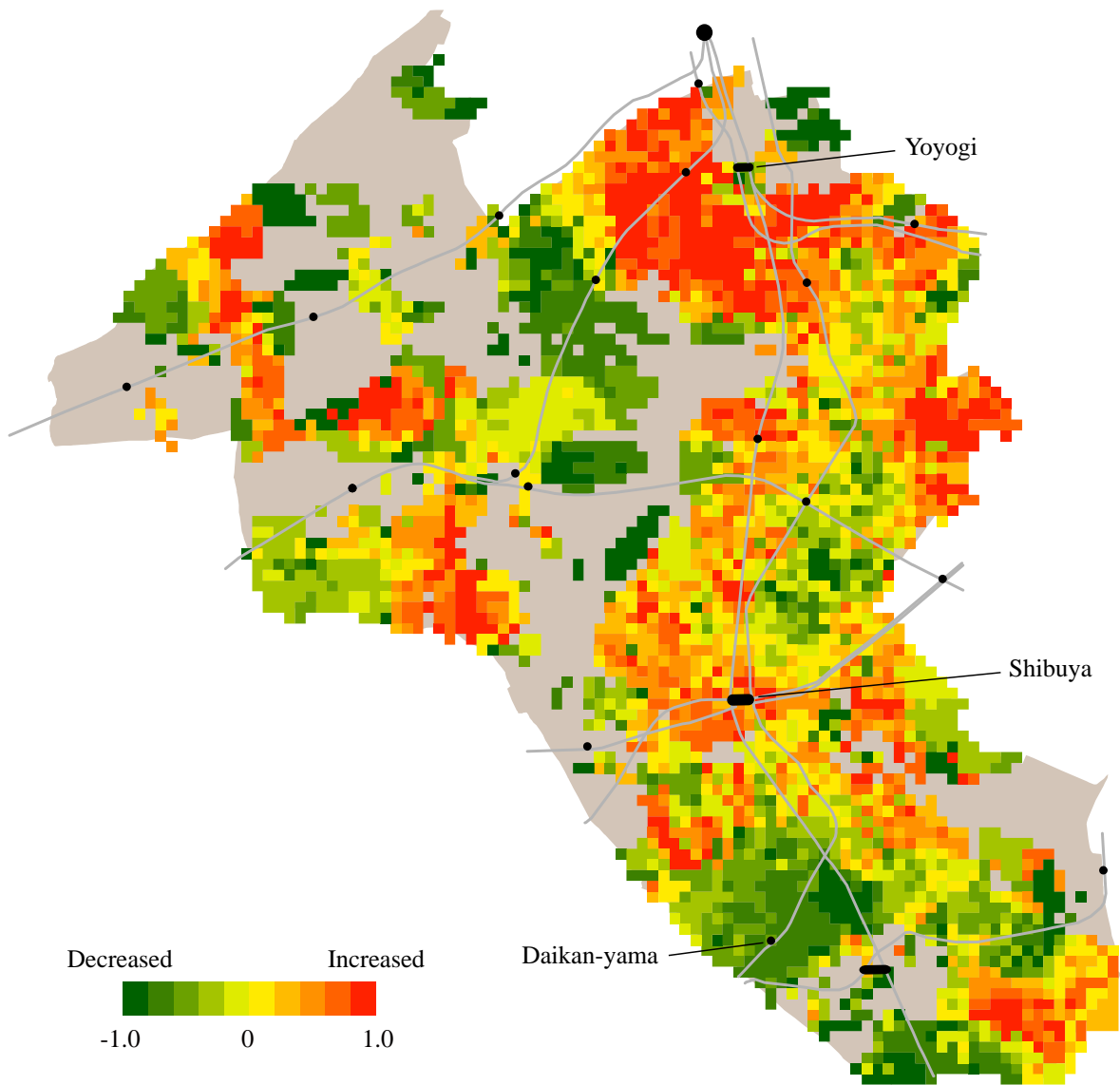


Figure 16 Lattice map of ρ of the openings of clothing stores.

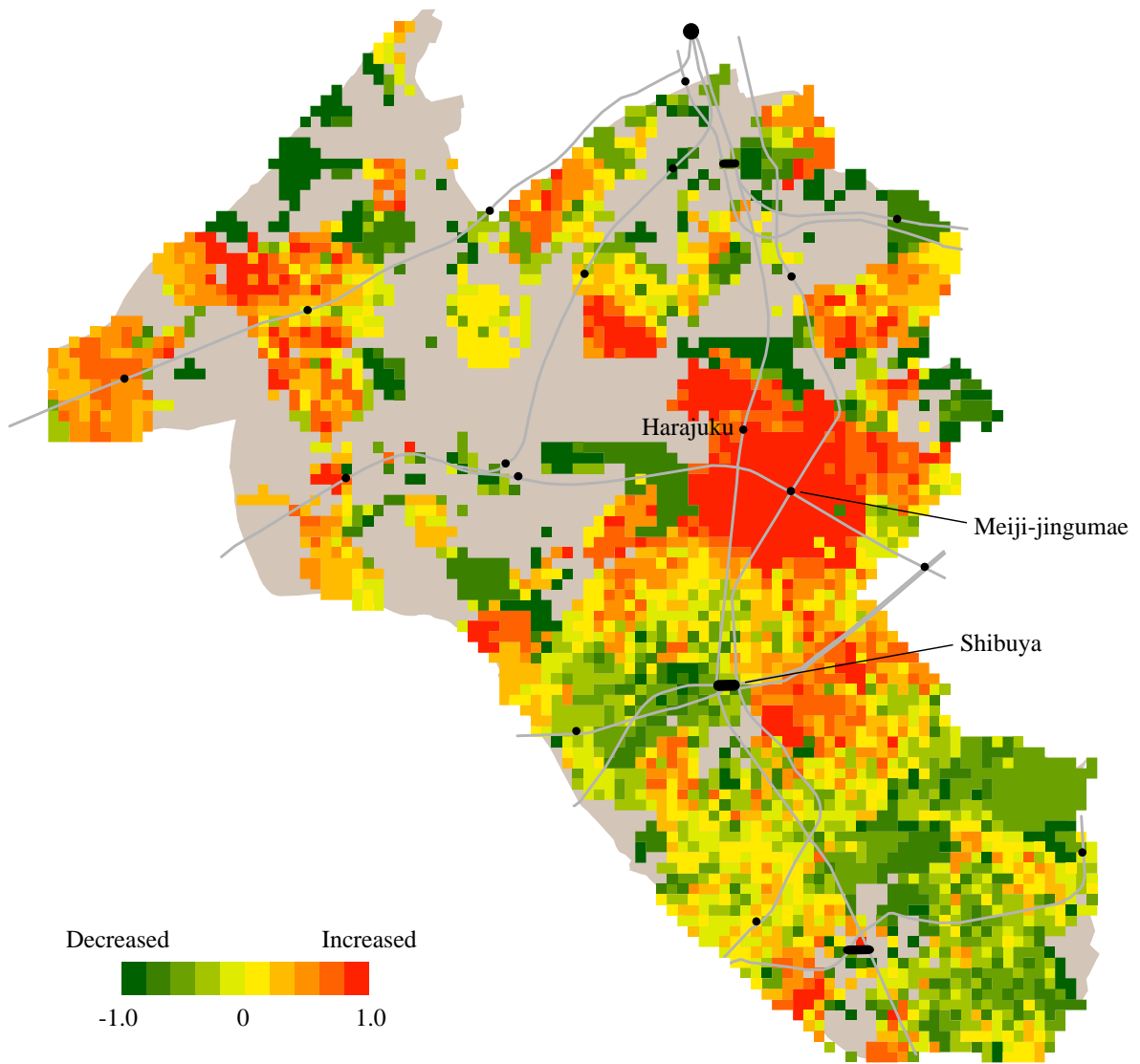


Figure 17 Lattice map of ρ of the openings of restaurants.

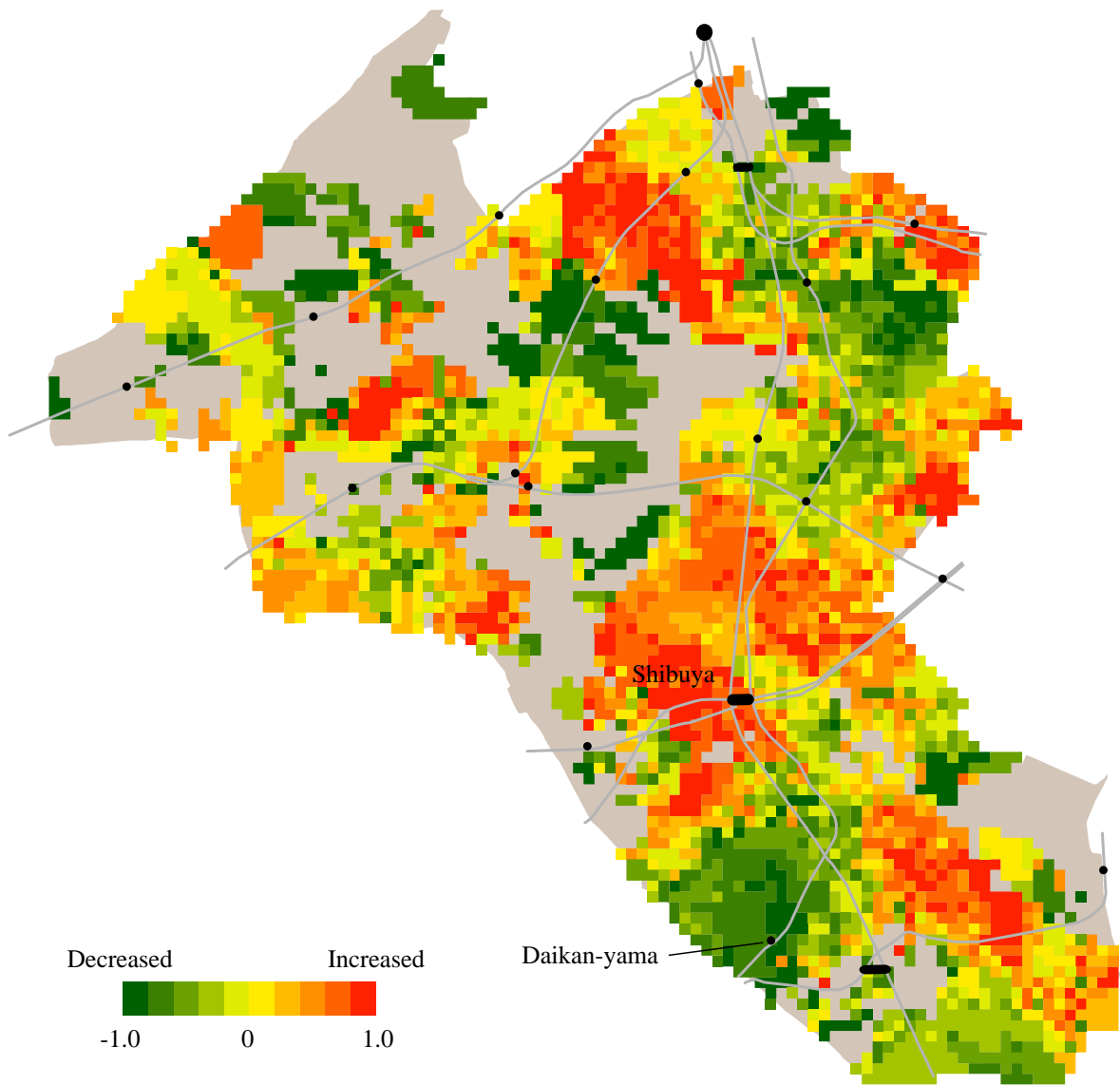


Figure 18 Lattice map of ρ of the closures of clothing stores.

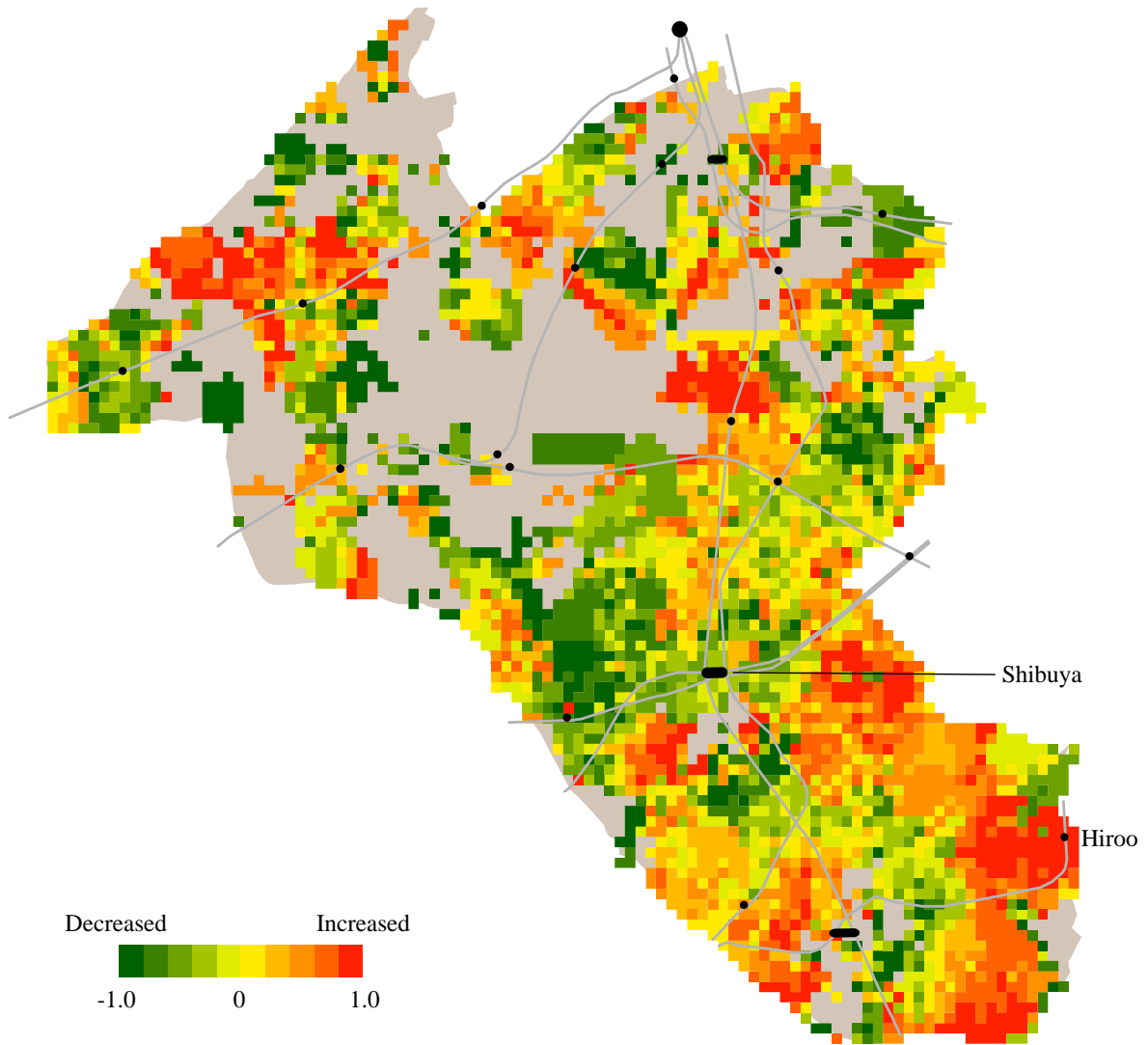


Figure 19 Lattice map of ρ of the closures of restaurants.

5. Concluding discussion

New method for analyzing the appearance and disappearance of points was developed. Four measures $\alpha_A(\mathbf{x})$, $\alpha_D(\mathbf{x})$, $\alpha_A^T(\mathbf{x})$, and $\alpha_D^T(\mathbf{x})$ were defined that indicate the intensity of spatial and temporal patterns of events. Lattice map visualizes the spatial distribution of these measure, which is effective for grasping the overall picture and regional variation of event pattern. Circle map is useful for detecting distinctive local patterns that may not be easily detectable in lattice map. The proposed method was applied to the analysis of shops and restaurants in Shibuya, Tokyo. The results supported the technical soundness of the method as well as revealed spatial and temporal patterns that are not easily detectable by existing methods.

One strength of our method is that it incorporates a statistical framework. Lattice map is

generated based on the maximum likelihood approach, which is different from the grid map that simply indicates the ratio of events. Another strength is that lattice and circle maps explicitly visualize the relationship between appearances and disappearances. These maps help us grasping the spatial and temporal relationship between these events.

Unlike scan statistics, the proposed measures are not statistically tested. This is primary because our focus is on the exploratory visual analysis of event pattern rather than its strict evaluation. Understanding of the overall and local pattern and variation is an important first step in exploratory analysis. However, we do not claim that statistical tests are not necessary. In circle map, a statistical test can be performed by using Monte Carlo simulation as is done in scan statistics. This test, unfortunately, cannot be completed in an acceptable time in our program written in C++. Though we can reduce computing time by decreasing lattice density, it may degrade the quality of analysis. Faster algorithm or efficient test procedure is indispensable for statistical test.

This paper considers the event pattern of immovable points. We should extend the proposed method to treat movable points because they represent humans, animals, and birds whose movements are analyzed in various fields. Movable points have a wide variety of events such as start, stop, turn, hit, integration, and division. Relationship between multiple types of events need to be considered since they are closely related with each other. Moreover, these events are also related to the movement of points. Further development is necessary for analyzing the events of movable points.

Implementation of the proposed method as an extension of computer packages is also an important topic. QGIS and ArcGIS are widely used in many academic fields for which many extensions have been developed. R is popular not only in statistics but also in geography and epidemiology. Development of extensions for GIS and statistical packages needs to be considered in future research.

Acknowledgements

I would like to thank The NTT TownPage cooperation for providing the telephone directory data. This research was supported by JSPS KAKENHI Grant Numbers JP15H02967 and 16H01830.

References

- Andrienko N, Andrienko G (2006) *Exploratory analysis of spatial and temporal data: A systematic approach*. Springer Science & Business Media,
- Anselin L, Syabri I, Kho Y (2006) Geoda: An introduction to spatial data analysis. *Geographical Analysis* 38: 5-22
- Besag J, Newell J (1991) The detection of clusters in rare diseases. *Journal of the Royal Statistical Society. Series A (Statistics in Society)*: 143-155
- Bithell J (1991) Estimation of relative risk functions. *Stat Med* 10: 1745-1751
- Bivand RS, Pebesma EJ, Gómez-Rubio V, Pebesma EJ (2008) *Applied spatial data analysis with r*. Springer,

- Boots B, Csillag F (2006) Categorical maps, comparisons, and confidence. *Journal of Geographical Systems* 8: 109-118
- Carolina A, Antunes L, KjÃ A (2017) Mortality in danish swine herds: Spatio-temporal clusters and risk factors. *Preventive Veterinary Medicine*
- Chen J, Roth RE, Naito AT, Lengerich EJ, Maceachren AM (2008) Geovisual analytics to enhance spatial scan statistic interpretation: An analysis of us cervical cancer mortality. *Int J Health Geogr* 7: 1
- Clayton D, Kaldor J (1987) Empirical bayes estimates of age-standardized relative risks for use in disease mapping. *Biometrics*: 671-681
- Conley J, Gahegan M, Macgill J (2005) A genetic approach to detecting clusters in point data sets. *Geographical Analysis* 37: 286-314
- Costa M, Assunção R (2005) A fair comparison between the spatial scan and the besag–newell disease clustering tests. *Environmental and Ecological Statistics* 12: 301-319
- Cronie O, Van Lieshout MNM (2015) A j - function for inhomogeneous spatio - temporal point processes. *Scandinavian Journal of Statistics* 42: 562-579
- Davies TM, Hazelton ML, Marshall JC (2011) Sparr: Analyzing spatial relative risk using fixed and adaptive kernel density estimation in r. *Journal of Statistical Software* 39
- Dawson J (2012) *Retail geography (rle retailing and distribution)*. Routledge,
- Dent BD (1999) *Cartography-thematic map design*.
- Diggle PJ, Chetwynd AG, Häggkvist R, Morris SE (1995) Second-order analysis of space-time clustering. *Statistical methods in medical research* 4: 124-136
- Fernando W, Ganesalingam S, Hazelton M (2014) A comparison of estimators of the geographical relative risk function. *Journal of Statistical Computation and Simulation* 84: 1471-1485
- Fernando WS, Hazelton ML (2014) Generalizing the spatial relative risk function. *Spat Spatiotemporal Epidemiol* 8: 1-10
- Finkelshtein D, Kondratiev Y, Kutoviy O (2012) Semigroup approach to birth-and-death stochastic dynamics in continuum. *Journal of Functional Analysis* 262: 1274-1308
- Fotheringham AS, Zhan FB (1996) A comparison of three exploratory methods for cluster detection in spatial point patterns. *Geographical Analysis* 28: 200-218
- Gabriel E (2017) Spatiotemporal point pattern analysis and modeling. In: SHEKHAR, S., XIONG, H., ZHOU, X. (eds) *Encyclopedia of gis*. Springer International Publishing, Cham
- Gabriel E, Diggle PJ (2009) Second - order analysis of inhomogeneous spatio - temporal point process data. *Statistica Neerlandica* 63: 43-51
- Gangnon RE, Clayton MK (2001) A weighted average likelihood ratio test for spatial clustering of disease. *Stat Med* 20: 2977-2987
- Glaz J, Naus JI, Wallenstein S, Wallenstein S, Naus JI (2001) *Scan statistics*. Springer,
- Greene SK, Peterson ER, Kapell D, Fine AD, Kulldorff M (2016) Daily reportable disease spatiotemporal

- cluster detection, new york city, new york, USA, 2014–2015. *Emerg Infect Dis* 22: 1808
- Han J, Zhu L, Kulldorff M, Hostovitch S, Stinchcomb DG, Tatalovich Z, Lewis DR, Feuer EJ (2016) Using gini coefficient to determining optimal cluster reporting sizes for spatial scan statistics. *Int J Health Geogr* 15: 27
- Hazelton ML, Davies TM (2009) Inference based on kernel estimates of the relative risk function in geographical epidemiology. *Biometrical Journal* 51: 98-109
- Holley R, Stroock D (1978) Nearest neighbor birth and death processes on the real line. *Acta mathematica* 140: 103-154
- Jacquez GM (1996) A k nearest neighbour test for space-time interaction. *Stat Med* 15: 1935-1949
- Kelley C (1995) Iterative methods for linear and nonlinear equations, siam, philadelphia, 1995. *MR 96d* 65002
- Kelsall JE, Diggle PJ (1995) Kernel estimation of relative risk. *Bernoulli*: 3-16
- Knox E, Bartlett M (1964) The detection of space-time interactions. *Journal of the Royal Statistical Society. Series C (Applied Statistics)* 13: 25-30
- Kovalerchuk B, Schwing J (2005) *Visual and spatial analysis: Advances in data mining, reasoning, and problem solving*. Springer Science & Business Media,
- Kraak M-J, Ormeling F (2011) *Cartography: Visualization of spatial data*. Guilford Press,
- Kulldorff M (1997) A spatial scan statistic. *Communications in Statistics - Theory and Methods* 26: 1481-1496
- Kulldorff M (2001) Prospective time periodic geographical disease surveillance using a scan statistic. *Journal of the Royal Statistical Society: Series A (Statistics in Society)* 164: 61-72
- Kulldorff M, Feuer EJ, Miller BA, Freedma LS (1997) Breast cancer clusters in the northeast united states: A geographic analysis. *American Journal of Epidemiology* 146: 161-170
- Kulldorff M, Heffernan R, Hartman J, Assunção R, Mostashari F (2005) A space–time permutation scan statistic for disease outbreak detection. *PLoS medicine* 2: e59
- Kulldorff M, Hjalmars U (1999) The knox method and other tests for space - time interaction. *Biometrics* 55: 544-552
- Kulldorff M, Mostashari F, Duczmal L, Katherine Yih W, Kleinman K, Platt R (2007) Multivariate scan statistics for disease surveillance. *Stat Med* 26: 1824-1833
- Kulldorff M, Nagarwalla N (1995) Spatial disease clusters: Detection and inference. *Stat Med* 14: 799-810
- Lamigueiro ÓP (2014) *Displaying time series, spatial, and space-time data with r*. CRC Press,
- Lawson AB (2013) *Bayesian disease mapping: Hierarchical modeling in spatial epidemiology*. CRC press,
- Li X-Z, Wang J-F, Yang W-Z, Li Z-J, Lai S-J (2011) A spatial scan statistic for multiple clusters. *Mathematical Biosciences* 233: 135-142
- Møller J, Sørensen M (1994) Statistical analysis of a spatial birth-and-death process model with a view to modelling linear dune fields. *Scandinavian Journal of Statistics*: 1-19
- Mantel N (1967) The detection of disease clustering and a generalized regression approach. *Cancer Research* 27: 209-220

- Marshall RJ (1991) Mapping disease and mortality rates using empirical bayes estimators. *Applied statistics*: 283-294
- Moller J, Waagepetersen RP (2003) *Statistical inference and simulation for spatial point processes*. CRC Press,
- Naus JI (1965) Clustering of random points in two dimensions. *Biometrika* 52: 263-267
- Neill DB (2011) Fast bayesian scan statistics for multivariate event detection and visualization. *Stat Med* 30: 455-469
- Neill DB, Mcfowland E, Zheng H (2013) Fast subset scan for multivariate event detection. *Stat Med* 32: 2185-2208
- Openshaw S, Charlton M, Craft AW, Birch J (1988) Investigation of leukaemia clusters by use of a geographical analysis machine. *The Lancet* 331: 272-273
- Openshaw S, Charlton M, Wymer C, Craft A (1987) A mark 1 geographical analysis machine for the automated analysis of point data sets. *International Journal of Geographical Information System* 1: 335-358
- Ortega JM, Rheinboldt WC (1970) *Iterative solution of nonlinear equations in several variables*. Siam,
- Ovaskainen O, Finkelshtein D, Kutoviy O, Cornell S, Bolker B, Kondratiev Y (2014) A general mathematical framework for the analysis of spatiotemporal point processes. *Theoretical ecology* 7: 101-113
- Oyana TJ, Margai F (2015) *Spatial analysis: Statistics, visualization, and computational methods*. CRC Press,
- Preston C (1975) Spatial birth and death processes. *Advances in applied probability* 7: 465-466
- Richardson S, Thomson A, Best N, Elliott P (2004) Interpreting posterior relative risk estimates in disease-mapping studies. *Environmental Health Perspectives* 112: 1016
- Robinson A, Morrison J, Muehrcke P, Kimerling A, Guptill S (1995) *Elements of cartography* 6th edn john wiley and sons. *New York*
- Scott DW (2015) *Multivariate density estimation: Theory, practice, and visualization*. John Wiley & Sons,
- Scott P (1970) *Geography and retailing*. Transaction Publishers,
- Silverman BW (1986) *Density estimation for statistics and data analysis*. CRC Press, Boca Raton
- Slocum TA, McMaster RB, Kessler FC, Howard HH (2009) *Thematic cartography and geovisualization*.
- Turnbull BW, Iwano EJ, Burnett WS, Howe HL, Clark LC (1989) Monitoring for clusters of disease; application to leukemia incidence in upstate new york. Cornell University Operations Research and Industrial Engineering,
- Van Lieshout M (2011) A_j -function for inhomogeneous point processes. *Statistica Neerlandica* 65: 183-201
- Van Lieshout MNM, Baddeley AJ (1996) A nonparametric measure of spatial interaction in point patterns. *Statistica Neerlandica* 50: 344-361
- Zhang Z, Assunção R, Kulldorff M (2010) Spatial scan statistics adjusted for multiple clusters. *Journal of Probability and Statistics* 2010

Appendix

This appendix maximizes an approximation of $L^T(Z, k, q)$ defined by in Equation (14). Omitting the constant terms in Equation (14), we take its logarithmic form:

$$l^T(Z, k, q) = \sum_i \left[a(Z_i) \log k q_i + \{n(Z_i) - a(Z_i)\} \log(1 - k q_i) + a(S_i - Z_i) \log q_i + \{n(S_i - Z_i) - a(S_i - Z_i)\} \log(1 - q_i) \right] \quad (\text{A } 1)$$

It is approximated as

$$l^T(Z, k, q) \approx \sum_i \left[a(Z_i) \log k q_i - k q_i \{n(Z_i) - a(Z_i)\} + a(S_i - Z_i) \log q_i - q_i \{n(S_i - Z_i) - a(S_i - Z_i)\} \right] \quad (\text{A } 2)$$

We solve the following system instead of Equations (15) and (16):

$$\begin{cases} \frac{\partial l^T(Z, k, q)}{\partial q_i} = 0 & (i \in I) \\ \frac{\partial l^T(Z, k, q)}{\partial k} = 0 \end{cases}$$

(A 3)

(A 4)

This system is rewritten as

$$\begin{cases} \frac{\partial l^T(Z, k, q)}{\partial q_i} = \frac{a(Z_i)}{q_i} - k \{n(Z_i) - a(Z_i)\} + \frac{a(S_i - Z_i)}{q_i} - \{n(S_i - Z_i) - a(S_i - Z_i)\} = 0 & (i \in I) \\ \frac{\partial l^T(Z, k, q)}{\partial k} = \sum_i \left[\frac{a(S_i - Z_i)}{k} - q_i \{n(S_i - Z_i) - a(S_i - Z_i)\} \right] = 0 \end{cases}$$

(A 5)

(A 6)

Equation (A 5) becomes

$$\frac{a(Z_i) + a(S_i - Z_i)}{q_i} = k \{n(Z_i) - a(Z_i)\} + n(S_i - Z_i) - a(S_i - Z_i),$$

(A 7)

and thus

$$q_i = \frac{a(Z_i) + a(S_i - Z_i)}{k \{n(Z_i) - a(Z_i)\} + n(S_i - Z_i) - a(S_i - Z_i)}.$$

(A 8)

Substitution of Equation (A 7) into Equation (A 6) yields

$$\begin{aligned}
\frac{\partial l^T(Z, k, q)}{\partial k} &= \sum_i \left[\frac{a(S_i - Z_i)}{k} - q_i \{n(S_i - Z_i) - a(S_i - Z_i)\} \right] \\
&= \sum_i \left[\frac{a(S_i - Z_i)}{k} - \frac{\{a(Z_i) + a(S_i - Z_i)\} \{n(S_i - Z_i) - a(S_i - Z_i)\}}{k \{n(Z_i) - a(Z_i)\} + n(S_i - Z_i) - a(S_i - Z_i)} \right] \\
&= 0
\end{aligned} \tag{A 9}$$

We approximate Equation (A 9) as

$$\begin{aligned}
\frac{\partial l^T(Z, k, q)}{\partial k} &\approx \sum_i \left[\frac{a(S_i - Z_i)}{k} - \frac{\{a(Z_i) + a(S_i - Z_i)\} \{n(S_i - Z_i) - a(S_i - Z_i)\}}{n(S_i - Z_i) - a(S_i - Z_i)} \right] \\
&= \frac{1}{k} \sum_i a(S_i - Z_i) - \sum_i \frac{\{a(Z_i) + a(S_i - Z_i)\} \{n(S_i - Z_i) - a(S_i - Z_i)\}}{n(S_i - Z_i) - a(S_i - Z_i)} \\
&= 0
\end{aligned} \tag{A 10}$$

Solving Equation (A 10), we obtain

$$\frac{1}{k} \sum_i a(S_i - Z_i) = \sum_i \frac{\{a(Z_i) + a(S_i - Z_i)\} \{n(S_i - Z_i) - a(S_i - Z_i)\}}{n(S_i - Z_i) - a(S_i - Z_i)}. \tag{A 11}$$

$$k = \frac{\sum_i a(S_i - Z_i)}{\sum_i \frac{\{a(Z_i) + a(S_i - Z_i)\} \{n(S_i - Z_i) - a(S_i - Z_i)\}}{n(S_i - Z_i) - a(S_i - Z_i)}}. \tag{A 12}$$

Substitution of Equation (A 11) into Equation (A 8) yields

$$\begin{aligned}
q_i &= \frac{a(Z_i) + a(S_i - Z_i)}{k \{n(Z_i) - a(Z_i)\} + n(S_i - Z_i) - a(S_i - Z_i)} \\
&= \frac{a(Z_i) + a(S_i - Z_i)}{\frac{\{n(Z_i) - a(Z_i)\} \sum_j a(S_j - Z_j)}{\sum_j \frac{\{a(Z_j) + a(S_j - Z_j)\} \{n(S_j - Z_j) - a(S_j - Z_j)\}}{n(S_j - Z_j) - a(S_j - Z_j)}} + n(S_i - Z_i) - a(S_i - Z_i)} \\
&= 0
\end{aligned} \tag{A 13}$$

We use Equations (A 12) and (A 13) as initial values of k and q_i 's in the iterative process to solve Equations

(15) and (16).